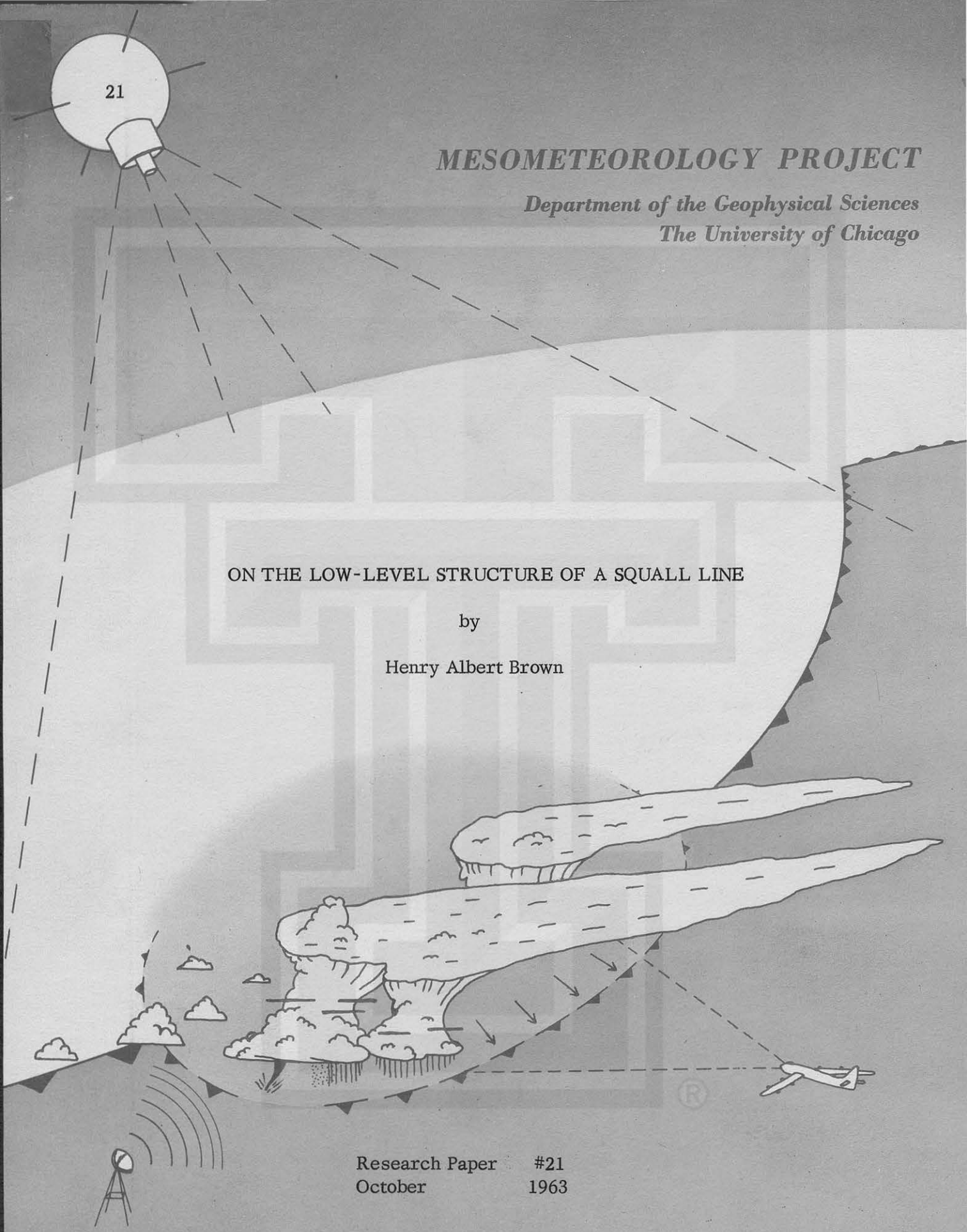

MESOMETEOROLOGY PROJECT

Department of the Geophysical Sciences
The University of Chicago

ON THE LOW-LEVEL STRUCTURE OF A SQUALL LINE

by

Henry Albert Brown

Research Paper #21
October 1963

MESOMETEOROLOGY PROJECT -------- RESEARCH PAPERS

1. Report on the Chicago Tornado of March 4, 1961 - Rodger A. Brown and Tetsuya Fujita *

2. Index to the NSSP Surface Network - Tetsuya Fujita *

3. Outline of a technique for Precise Rectification of Satellite Cloud Photographs - Tetsuya Fujita *

4. Horizontal Structure of Mountain Winds - Henry A. Brown *

5. An Investigation of Developmental Processes of the Wake Depression Through Excess Pressure Analysis of Nocturnal Showers - Joseph L. Goldman *

6. Precipitation in the 1960 Flagstaff Mesometeorological Network - Kenneth A. Styber *

7. On a Method of Single- and Dual-Image Photogrammetry of Panoramic Aerial Photographs - Tetsuya Fujita (To be published)

8. A Review of Researches on Analytical Mesometeorology - Tetsuya Fujita

9. Meteorological Interpretations of Convective Nephsystems Appearing in TIROS Cloud Photographs - Tetsuya Fujita, Toshimitsu Ushijima, William A. Hass, George T. Dellert, Jr.

10. Study of the Development of Prefrontal Squall-Systems Using NSSP Network Data - Joseph L. Goldman

11. Analysis of Selected Aircraft Data from NSSP Operation, 1962 - Tetsuya Fujita

12. Study of a Long Condensation Trail Photographed by TIROS I - Toshimitsu Ushijima

13. A Technique for Precise Analysis of Satellite Date; Volume I - Photogrammetry - (Published as MSL Report No. 14) - Tetsuya Fujita

14. Investigation of a Summer Jet Stream Using TIROS and Aerological Data - Kozo Ninomiya

15. Outline of a Theory and Examples for Precise Analysis of Satellite Radiation Data - Tetsuya Fujita

* Out of Print

(Continued on back cover)

MESOMETEOROLOGY PROJECT

Department of the Geophysical Sciences

The University of Chicago

ON THE LOW-LEVEL STRUCTURE OF A SQUALL LINE*

by

Henry Albert Brown

RESEARCH PAPER #21

* Reprinted from Mesometeorological Study of Selected Areas in the United States, Final Report to the U. S. Army Signal Corps under Contract No. DA 36-039 SL - 88932.

Table of Contents

On the Low-Level Structure of a Squall Line

Henry Albert Brown

Abstract

The design of a field operation which took place during the month of May, 1962, in the Dallas-Fort Worth, Texas, area is described. The purpose of the operation was to obtain moisture, temperature, and wind observations in the low-levels of a squall line. The Cedar Hills television tower (1420') proved to be an ideal location for such an operation. In addition to the instrumentation already mounted on the tower, temperature and moisture were sampled continuously at six levels. Surrounding the tower, small scale and mesoscale networks were maintained for a horizontal capability.

The operational results are cataloged in the analysis of a squall line which passed the area on May 28-29, 1962. High-level time and space sections revealed the environmental conditions, while low-level sections of wind, moisture, and temperature revealed the structure of the squall line. Results of the study indicated that the moisture anomaly, referred to as a "humidity dip", increases in magnitude with height. Another feature noted was the existence of a low-level moisture maximum located just ahead of the squall line.

1. INTRODUCTION

Studies of convective activity have been carried out over many years utilizing data obtained by special devices or networks. Examples include the early work by Suckstorff (1935) in which the conversion from time to space at a single station was presented as a means of physical representation of phenomena. The case studies by Byers (1942) of the data collected by the Muskingum Soil Conservation Network revealed the origin of convective systems from small areas and the production of meso-

scale cold air masses by thunderstorm cooling. Analyses of the Lindenberg network data, Koschmieder (1955), although mainly concerned with the abrupt wind maximum that accompanies a thunderstorm passage also contained detailed analyses of temperature, humidity and precipitation. The establishment of the Thunderstorm Project Network in 1946 and 1947 led to the collection of extremely detailed data on thunderstorms through the operation of a small-mesh (2 miles), small-area (160 square miles) surface network, which included rawinsonde stations capable of serial ascents, radar and aircraft. Analyses of these data by Newton (1950) and Fujita (1957) led to a more complete understanding of the three-dimensional structure of squall lines. The establishment of the Weather Bureau National Severe Storms Project in the central United States produced surface data from a larger-mesh (30 miles), larger-area (250,000 square miles) network during the season of greatest convective activity. These network observations, together with radar observations, presented the basis for the development of the field of mesometeorology through the detailed studies of Tepper, et. al. (1954), Fujita (1955), Fujita, Newstein and Tepper (1956) and Tepper (1957).

The need for the design of a network which would be capable of resolving many of the problems encountered by the mesoanalyst was first recognized by the USASRDL who, in 1959 through contract with the University of Chicago Mesometeorology Project, initiated such a project design. The final designs, Fujita and Brown (1960), which consisted of coastal, plains and mountainous networks, contained, in essence, three interwoven networks: a large-mesh (30-40 miles), large-area (120,000 square miles) network, referred to as the α network; a medium-mesh (7 miles), medium-area (2400 square miles) network, referred to as the β network; and the possibility of a third smaller-scale smaller-mesh micro-network, referred to as the γ network.

The chance to apply some of the design criteria in the above report on a much smaller study was presented through a recent study made by Brown (1962) on the moisture field associated with squall lines. This report established the existence of a mesoscale anomalous moisture feature, the humidity dip, along the leading edge of a squall line. The dip was connected with other meteorological parameters in time and space and several explanations for the possible cause of the dip given. The im-

plications of the dip with respect to the squall line were noted and it was determined that knowledge as to the vertical extent of the dip was required for further research.

This report will outline, therefore, the design of the operational field study to accomplish this goal, the data sources and in addition will present some of the results obtained.

2. DESIGN OF THE FIELD OPERATION

Following the establishment of the need for certain types of measurements in the low-levels of squall lines, the USASRDL agreed to loan various instruments for a short-period field operation. The location of a new meteorological research tower, Stevens and Gerhart (1959), in the area of Dallas, Texas which had the capability of sensing temperature and wind on an almost continuous basis at twelve levels up to 1420 feet together with the rather dense existing surface observation network made this area a logical choice for the operation. The addition of moisture measuring devices on the tower was accomplished through the cooperation of the AFCRL, GRD and the EERL of the University of Texas.

The primary data source for the operation under University of Chicago maintenance included, Fig. 1, the instrumentation of the tower at six levels, 30', 150', 450', 750', 1050' and 1420', with hygrothermographs. The base and top of the tower were also equipped with microbarographs. Surrounding the tower was a triangular network, the locations of which had been established by the Micrometeorology Section of the A. and M. College of Texas. These sites were instrumented by the University of Chicago with hygrothermographs, microbarographs and continuous wind speed and direction recorders. To the north, west and south of the tower and the γ network, a β network which consisted of microbarographs was established and operated by the University of Chicago. These stations were so arranged that they merged with the existing Weather Bureau, Air Force and Navy stations to extend the network over a much larger area. Surrounding the β and the γ networks was the larger area NSSP α network which was maintained by the Weather Bureau. Visual cloud surveillance of the area during the daylight hours was achieved by time-lapse photography.

Additional data sources for the operation included the wind and temperature

measurements from the television tower, which had been placed on one-minute integration periods when a squall line passage was imminent. The A. and M. College of Texas maintained and operated two micrometeorology vans in the area. One was located at the base of the television tower, the other a short distance to the southeast. Surface observations and additional recorded data were made available by the weather stations in the area that were operated by the Weather Bureau, (Carter Field and Love Field), the Air Force (Carswell AFB), the Navy (Hensley NAS), and the Federal Aviation Agency (Meacham Field). The rawinsonde and the radar observations made by the Fort Worth Weather Bureau Station were also an extremely valuable addition to the study.

3. INSTRUMENT CALIBRATION

Calibration of the β and γ network instruments was essential in order to determine the vertical and horizontal structure of the moisture and other related fields. Thus, the wind instruments were calibrated in the laboratory for system characteristics, e.g., amplifier, wind direction. In the field, comparative runs, Fig. 2, were made over varying periods of time, in order to sample varying conditions of wind speed. Checks then indicated consistencies and inconsistencies in the response of two instruments to the same forcing function. Due to the excellent maintenance work done at the A. and M. College of Texas laboratories the instruments showed excellent agreement in the field tests. The wind directions were oriented in the field using geological survey-type compasses and magnetic deviations were taken into consideration. The masts and the booms on which the instruments were mounted were of a design that made possible quick, accurate and comfortable orientation.

The microbarographs were calibrated for relative variations of pressure by twenty four hour runs of all instruments under the same conditions. The responses of the instruments were then checked for consistency and corrections made for instruments which amplified any atmospheric pressure change. The response of the instruments over larger variations of pressure would have been an additional aid to the accuracy of the analyses; however, a pressure chamber was not available at the site. The transportation of the microbarographs into a canyon was not possible, as

it was in the Flagstaff operation of 1961. The tower itself would be ideal for an approximate 50 mb variation but the size of the elevator precluded the simultaneous transportation of twelve microbarographs. It was,thus, considered that the twenty four hour check at the beginning and end of the operation would be sufficient to point out any important instrument discrepancies.

The hygrothermographs were checked prior to installation in the field in a crude but effective manner. The major effort was to bring all instruments into the same test environment for the same duration of time. In order to achieve this goal all instruments (nine) were placed on a rolling table and allowed to come into equilibrium with the environment room (77.4°F, 66%). They were then wheeled into the cold chamber (48.5°F, 88%) and allowed to remain for approximately one hour. After this time they were wheeled back into the environment room (78.0°F, 65%) and the recovery curves noted. It should be noted that all recording instruments, microbarographs and hygrothermographs, were equipped with 29 hour gears, thus equating one centimeter of chart space to one hour. The responses of the instruments to this approximation of a black forcing function were then studied and the six which showed the best agreement were placed on the tower. The remaining three were placed in the Y network. Since all nine instruments were new, there was not too great a deviation of the responses.

Prior to their installation in the field and following their return from the field, all hygrothermographs were subjected to the same twenty four hour test of similar envrionment conditions as the microbarographs. While in the field the hygrothermographs were checked by means of a sling psychrometer, the television tower instruments being checked most frequently.

Time consistency of all instruments was insured to a great degree by daily time checks of the observers with a central location, namely the U. of Texas television tower system time. It was thus hoped that the comparison of the fast response temperature system data with the slow response hygrothermographs would allow for another check on the temperature variations recorded.

4. CONSTRUCTION OF BASE MAPS, NOMOGRAPHS AND TABLES

In order to facilitate the field operation and allow for some flexibility in the

operation of the network, it was decided to attempt some field analysis of the incoming data and correct for obvious errors in instruments and placements. The daily servicing of all instruments and collection and inspection of data at a central location was augmented by "trouble-shooting" tactics when an obvious malfunction was noted and telephoned into the central location. The analysis of the incoming data was effected on a variety of charts which were constructed especially for the area under study.

For the large-scale study of conditions which would be considered potential squall line producers, a base map of scale 1: 5,000,000 was utilized. For more detailed studies of atmospheric features, charts in the scales of 1: 2,000,000, 1: 1,000,000, and 1: 250,000 were used. The locations of the β and γ network stations were effectively made through a field survey utilizing geological survey maps and a pronounced checkpoint when available, namely the 1400' television tower in most cases.

The plotting of the television tower data presented a problem until a low-level thermodynamic diagram, which is based on coordinates of - RTlnp and ln RT, was constructed. This diagram, the Refsdal (1935, 1937) aerogram, presents several features which make it most suitable for the analysis of data of the type collected. The principal feature is that through the particular choice of the coordinates, a fixed height-coordinate system can be placed on the diagram. Thus, the data, which is determined at a constant z rather than in terms of p, can be plotted and all related thermodynamic computations can be made on the assumption that the surface pressure, over sufficiently small periods of time, varies an insignificant amount. In this case, reference to Fig. 3 indicates that the horizontal, or ground elevation line coincides with the 984 mb surface, the Standard Atmosphere pressure for the elevation of the station.

In addition to the isolines of pressure, calculation and construction of isolines of potential temperature, θ, (^{o}K) saturation mixing ration, r, (gm/kg) and equivalent potential temperature, θ_e (^{o}K) or pseudoadiabatic lines. The diagrams in the latter part of this report and the conversions from relative humidity to mixing ratio were effected through use of this chart.

Occasionally there were needs for the rapid computation of divergence and vor-

ticity. Since the r network was a small fixed triangular grid and since the analysis of winds over the area without a larger area of data coverage could be quite subjective, it was decided to compute tables, Bellamy (1949), for the computation of divergence and vorticity based on the assumption of a linear wind distribution between points. It is recognized that the validity of the assumption that the average of the values of the wind at two sites is the same as the average value of the wind between the two sites depends on the variations of the wind field in a smaller space scale. However, lacking more detailed information it is felt that the values obtained can be considered representative within the triangle. The tables thus obtained, Fig. 4, 5 and 6, produce numbers with dimensions (hr^{-1}) which can be obtained upon entrance with values of wind direction and speed. Note that the sign of the number is determined by the wind direction. The sum of the three numbers then gives the value of divergence within the triangular network for the given values of wind speed and direction. It should also be noted that the tables apply to any time-averaged wind values which are calculated, and produce any time-averaged value of divergence which is desired. Examples are given in a later section of this report. For computation of the vorticity, the tables should be entered with wind speed and a wind direction which is 90 degrees greater than the reported one.

5. OPERATIONAL RESULTS

A. PERIOD OF OPERATION

The period selected for the field operation was the month of May, 1962. The primary reason for the choice of this period was the fact that an intensive severe storm research operation was being conducted by the Weather Bureau at that time. The advantages gained by the choice of this time in terms of extra rawinsonde ascents, increased alertness of the network personnel, aircraft reconnaissance flights, etc., was almost offset by the anomalous lack of thunderstorms in the area for that period of the year. The University of Chicago operation was in full progress by May 2, 1962. The period of no -thunderstorm occurrence extended from April 30, until May 22, 1962.

It would, however, be erroneous to imply that the early part of the month was a loss in terms of research potential. Under what might be termed quiescent conditions in that area, e.g., 1) moderate southeasterly winds at the surface, decreasing at night, 2) low stratus clouds moving into the area in the early morning and dissipating in the late morning, 3) buildup of a low-level jet in connection with the low-level temperature inversion and 4) scattered cumuli in the early afternoon, some extremely interesting temperature and moisture data were collected on the tower, especially in the upper levels, 750'to 1400'. It is anticipated that this data will be the subject for further study.

Following a thunderstorm occurrence on the 22nd of May, three additional squall line passages occurred before the operation was terminated on June 2, 1962. In all cases the University of Texas tower system had been placed on one-minute integration operation. The squall line to be discussed in the following sections occurred on May 28-29.

B. SYNOPTIC SITUATION

The synoptic situation that prevailed during the period of squall line development and propagation through the network can be discussed by reference to Fig. 7-10. Throughout the early part of May and also on the 28th and 29th the operational area was located on the western side of an intense large-scale anticyclone. The upper-level conditions will be discussed in the next section, however it can be indicated that the area was in a condition of potential instability. To the west, the conditions consisted of an almost stationary cold front extending southwest from Kansas across the southeastern corner of Colorado and into New Mexico. A dry front, extending almost north-south through the Oklahoma and Texas Panhandles and into southwest Texas, began to advance to the east on the morning of the 28th initiating severe storms in the warm moist air of central Oklahoma and Texas. The charts, Fig. 7-10, indicate the progress and the development of the mesosystems as they moved into eastern Oklahoma and Texas. The conditions that prevailed were quite similar to a case, Brown (1958), in which the severe storm area was essentially a series of organized mesosystems which had originated at different times but which were lined

up in such a manner that the severe storm area appeared to be a macroscale phenomenon. Thus, the squall line was composed of individual mesosystems whose ages varied from old or dissipating in the north, through mature in the central section, to new or developing in the south. The position of the network area with respect to the severe weather at the four map times, 1800, 2100, 0000 and 0300 CST can be seen in the figures.

C. HIGH-LEVEL TIME AND SPACE SECTIONS

The structure of the atmosphere prior to, during and following the severe storm activity can be represented by means of z-t or x-z cross-sections. The special raw-insonde ascents made at Fort Worth, Texas were plotted on a modified skew-T thermodynamic diagram and then transferred to the time section shown in Fig. 11. The temperature and dew-point curves are indicated by the dash-dot and dash lines. Computation of the Showalter Stability Index through the 1730 sounding indicated instability values on the order of 3 to 5 degrees. The low-level moisture inversion prior to the passage of the squall line is quite evident and shows some lifting with time. The 2330 CST sounding is indicative of the squall line zone as evidenced by the cooling in the lower layer and the marked warming in the upper. This is also shown by the temperature and potential temperature analyses through the upward bulge in the isotherms and the tropopause and the downward dip in the isolines of potential temperature. The 0530 CST sounding signifies the return to a more normal temperature-moisture distribution for that time of the day.

Space sections along a line from Shreveport through Fort Worth to Midland were constructed for two observation times, 1800 and 0000 CST. At the earlier time the squall line was located between Midland and Fort Worth, at the later time, between Fort Worth and Shreveport. The space sections do not indicate an upward bulge in the tropopause of the same scale as the time section. This is possibly due to the larger gap between the observation stations in space, but more probably due to the validity of a simple advection model of the atmosphere. If we consider the shift from time to space coordinates in Fig. 11, with a conversion of one hour equal to 30 miles per hour, approximately the speed of the squall line, then the coordinates

of Fig. 11, Fig. 12 and 13 are essentially the same, and the above comparisons can be made. Re-examination of the time section as a space section and the synoptic charts, Fig. 7-10, reveals that a sounding made at 2030 CST and again at 0230 CST would have been an excellent addition to the study in terms of a proximity sounding at the leading and trailing edge of the squall line system.

D. LOW-LEVEL TIME SECTIONS

The time sections of temperature and humidity recorded by the tower and the network instruments are of great interest since one of the goals of this study was to determine the moisture and temperature variation at various levels through squall lines. The determination of the vertical extent of the humidity dip was an additional aim of the operation.

The time variations of temperature and humidity at six lower levels for a period which encompasses the squall line are shown in Fig. 14a and 14b. The most striking temperature feature first noted is the familiar drop associated with the onset of the squall. It should be mentioned that time in the figures increases to the left in order to present a qualitative space representation to the system, which is moving from the west to the east. The temperature variations can be separated into three segments for descriptive purposes. The pre-squall temperatures present an adiabatic lapse rate with height and very little time change at any level. The squall zone (from 2130 to 0330 CST) is characterized by the practically simultaneous drop in temperature at all levels followed by a rapid recovery of temperature at the highest levels and several warming periods on the order of thirty minutes while the lowest levels remained relatively steady and undisturbed. The post-squall zone is marked by a rapid warming at the upper levels and the establishment of a strong inversion. The onset of the so-called post-squall zone is also characterized by a sudden drop in pressure, which is recognized through the analyses to be the wake low. It is quite conceivable that reports of sudden warmings behind squall lines are simply indications of the penetration of these temperature rises to the surface.

The humidity traces, Fig. 14b, present a much more complicated variation with time than does the temperature. The feature which shows up most clearly is the

humidity dip which occurred at about 2125 CST, or at the same time as the temperature drop and squall line onset. Upon close examination of the dip it can be seen that the minimum humidity reached in the dip was approximately 70% at all levels; thus, even for an isothermal lapse rate, the mixing ratio decreases with height at the lowest point of the dip. Since the moisture field can be more clearly represented by conversion to mixing ratios, the utilization of the low-level thermodynamics diagram presented data which will be shown in a later section. However, it can be stated here that the dips in mixing ratios were of greater magnitude at the higher levels of the tower than at the lower levels; thus, the conclusion may be drawn that the moisture anomaly does indeed intensify with height.

In order to illustrate the fact that the humidity dip was a mesoscale feature in this case and not a local phenomenon, time sections were prepared for the r network stations, Fig. 15. In addition, pressure traces were also shown in order to better outline the zone of disturbance. It is quite clear that the humidity dip was a characteristic of the squall line at this stage of the squall development. The examination of surface station data, following the analysis of data of the type collected on the tower, is disquieting upon consideration of how little can be shown about the atmospheric conditions only a few hundred feet above the surface, by an analysis of surface data.

Following the examination of the hourly mesoanalysis and the time sections of the various tower levels and the r network, it was decided to analyse in more detail the tower data, Fig. 16-18. In order to increase the information previously given on low-level squall line structure, unedited wind data from the University of Texas instrument system were plotted at the twelve observing levels at half-hour intervals shown in the figures. Superimposed on the winds are isolines of temperature and mixing ratio. The temperature and moisture analyses are derived from 10-minute observations of the six University of Chicago instruments. The first chart, Fig. 16, which is representative of the pre-squall zone is characterized by wind directions which are predominantly southerly and show little variation with height or time. The speeds, in general, increase with height if the uppermost level is neglected. Because of the tower superstructure at this level, Gerhart (1962), the winds are considered to be unrepresentative. The temperature field, as previously noted in Fig. 14a,

illustrates an essentially diurnal decrease with time. The temperature variation between top and bottom of the tower is on the order of eight degrees. Examination of the diagram, Fig. 3, reveals this to be the adiabatic lapse rate. The time variations at the lower levels are due to cloud shadows.

The examination of the moisture field of the pre-squall zone reveals an interesting feature. In the early afternoon, 1300 CST, the moisture variation with height can be represented by a constant mixing ratio of about 15 gm/kg. With the passage of time, however, mixing ratio values increased at the middle levels, 450' and 750', more rapidly than at the upper and lower levels, 1420' and 30'. Thus, by 2000 CST, an hour and a half before the squall line passage, the moisture field indicated a maximum of 19 gm/kg at 750' with values dropping off to approximately 17 gm/kg at 1420' and 30'. The validity of this feature, as far as instrument spacing is concerned, is apparent since it is much larger in scale than the measuring grid. The presence of such a feature in the pre-squall zone, in an approximately adiabatic environment and with little wind speed variation, should be verified in other cases in order to determine whether it is a common occurrence. The implications of such a feature acting as a low level moisture source to the squall line would also require the elimination of the possibility of the feature being local rather than general in nature.

The squall zone, Fig. 17, is marked by the abrupt shift in wind direction at about 2125 CST and continues through the period of westerly winds at the upper levels and the period of shifting winds, from northwest through west into south, at the lower levels until approximately 0400 CST. There appear to be no striking cases of low-level jets in this zone. A weak jet-like maximum occurs between the 750' and 1050' level from 0200 until 0300 CST. Between 0300 and 0400 wind speeds decreased at all levels marking the wind direction shift at all levels to a more southerly direction. The temperature field of the squall zone is marked by the cold core of the main downdraft in the leading portion of the zone. Other features are the warm pockets of temperature at the middle levels. These were also noted on Fig. 14a. One of the most remarkable features of the temperature field is the rapid warming that took place between 0300 and 0400 at the upper levels. This warming coincided with the surface pressure drop (or wake low passage). Following this warming, what has been described

as the post-squall zone of the disturbance is apparent. It may be noted here that the rapid warming, which is evidently connected with subsidence at the upper levels since the penetration does not extend to the surface, coincided with surface wind divergence changing rapidly to convergence. This is in agreement with the study, Brown (1962), on the vertical motion field in a squall line. The moisture field of the squall zone is characterized by the abrupt change in the leading edge of the squall and the appearance of the mixing ratio dip which increases in magnitude with height. If the speed of the system is 30 miles per hour, then the conversion of time to space would indicate that the dip is on the order of 7.5 to 15 miles wide. This is in good agreement with other findings, Brown (1962).

The post-squall zone, Fig. 18, is characterized by southerly winds and no pronounced level of maximum winds. The low-level jet was apparently just above the height of the tower. An indication of this can be seen through the location of 40 mph wind speeds from 900' to 1421' between 0600 and 0700 CST. The temperature field which began the period with strong inversion conditions ended the period with a return to adiabatic conditions. The lifting or dissipation of the inversion shows an interesting wave-like formation. Examination of the actual traces, Fig. 14a, also reveals this feature. The moisture field in the post-squall zone is characterized by an apparent return to high mixing ratio values similar to the pre-squall zone. It should be mentioned that the dry front, noted in the mesoanalyses, Figs. 7-10, did not actually pass the network area during the period under study. Instead, it became stationary following its initiation of activity, then dissipated and reformed farther to the west on May 29.

The time variation of the network divergence of the surface wind field in the area of the r network was determined by using the tables, Fig. 4-6, constructed with a technique described by Bellamy (1949). The first computation, Fig. 19, was made using one-minute average winds at ten-minute intervals. Here again it is convenient to describe the features in terms of squall zones. The pre-squall zone is characterized by a convergent wind field which occasionally becomes non-divergent. The strong convergence noticed at 2130 is partially due to the fact that at that time the leading edge of the squall line was within the network. The strong divergence values occurred when the squall line had just passed the network. The divergence values

within the squall zone decreased following the initial peak and became convergent between 0100 and 0200. The return to divergent values is connected with the transition from the squall to the post-squall zone. The beginning of post-squall zone and the sudden warming at the upper levels, Figs. 14a and 17, at 0400 CST marks the abrupt change from divergence to convergence in the surface wind field. In order to compare various averages in the computation of the divergence fields, another series was prepared, Fig. 20, using ten-minute average winds every 15 minutes. The results, except for the decrease in the value of pre-squall convergence and some shift peaks in time, are essentially the same as those produced by the previous averaging process.

6. SUMMARY

In summary, the justification, planning, and operation of a field program for the attack on a certain parameter of an organized convective system have been given. The opportunity to test the design of a three-dimensional network with the capability of recording continuous time variations of various parameters was related and the descriptions of instruments used in the vertical and horizontal networks given. Methods of calibration were mentioned. The various map scales, tables, and nomographs utilized in the field operation and in the analysis of the data were detailed, and a case study which resulted from the operation was described.

The squall line which occurred in the Fort Worth-Dallas area on May 28-29 had been initiated along a dry front that extended almost north-south through central Texas and Oklahoma. High-level space and time sections revealed, in addition to the large-scale potentially unstable air and the apparent lifting of the tropopause surface in the squall area, the real need for greater space and time density of upper-level observations. Low-level time and space sections of pressure, temperature, moisture, wind and divergence obtained from the 1420' television tower and the β and γ networks revealed numerous interesting features. The existence of a low-level moisture maximum in a zone directly in front of a squall line was established. This moisture maximum which is not accompanied by a wind maximum or temperature inversion should be given more detailed study for the proof of its validity and the effect it may have on

the squall itself. The humidity (or mixing ratio, or dewpoint) dip occurred within the squall line, and it was shown that not only does the dip exist up to appreciable heights, but that it also increases in magnitude with height. The surface wind field was shown to be convergent prior to the squall line passage, divergent within the squall line and strongly divergent in the zone of the humidity dip, and convergent in the wake-low portion of the squall line. The rapid subsidence warming in the upper levels of the tower during the squall passage and the abrupt warming, almost to the surface, during the transition to the wake-low portion of the squall line gives an explanation to the sudden warmings that have been noticed at the surface following squall passages. Under a strong enough impulse these features could easily penetrate to the surface. An examination of the Fort Worth (Carter Field) telepsychrometer revealed such a warming at the surface during this particular squall. It was characterized by a sharp peak in the temperatures and an equally sharp increase in the wet bulb-dry bulb differences.

Although this report must be categorized as essentially a preliminary report on the data collected, it nevertheless demonstrates the need for continued detailed analysis. In addition, as shown above, the experience and results gained by the field operation and the analysis, have already indicated many improvements that can be made in future operations which may be concerned with this type of phenomenon. Even though, admittedly, hygrothermographs are not the precision type instrument which one might desire for such an undertaking, they would still be recommended as a low-cost, easily maintained, additional check on any system which consisted of fast-response devices. As a "mesoscale" instrument, it has proved quite valuable. Finally, the report has emphasized the potential of this type of field operation and combined study. Another study which should be initiated is the variation of temperature, moisture, and wind in the low-levels under nocturnal non-disturbed (i.e., by convective activity) conditions.

ACKNOWLEDGEMENTS

An operation which involves as many agencies as this one did is open to the error of omitting to acknowledge someone who made a significant contribution to its successful completion. If such omissions are made, they are accidental and do not reflect a lack of appreciation on the part of the author.

The University of Chicago: Dr. Tetsuya Fujita, the Director of the Mesometeorology Project who gave this operation his backing. Mr. Robbi Stuhmer and Mr. Stephen Graham, who produced most of the data plots.

USASRDL: Mr. Marvin Lowenthal, Contract Monitor, who effected the loan of the necessary instruments and otherwise gave encouragement and assistance to the project.

AFCRL-GRD: Dr. Morton Barad, Mr. Duane Haugen, and R. William P. Elliott for their cooperation in the establishment of the instruments on the television tower.

University of Texas: Dr. John Gerhart for placing his facilities at my disposal. Mr. William Mitcham, for his aid in the placing of the instruments and shelters on the tower.

A. and M. College of Texas: Dr. William Clayton, who placed his facilities at the author's disposal and for loaning various instruments which were vital to the operation.

USWB-NSSP: Dr. Chester W. Newton, for arranging for the loan of the network data collected during this period by the NSSP.

Hill Tower Co.: Mr. Cliff Ellis, Tower Engineer, for servicing the tower instruments.

USWB Carter Field: Mr. Oral J. Knarr, MIC, for his cooperation and assistance, Mr. Kirby Powell, Mr. George Carranza, and Mr. Gary Hartley for servicing the network instruments.

Final mention should be made of the cooperation that was given and interest shown by the Commanding Officers and Officials-in-Change of the Base Weather Station, Carswell AFB; FAA Station, Meacham Field; USWB Station, Love Field; and Base Weather Station, Hensley NAS.

REFERENCES

Bellamy, J. C., Jr., 1949: Objective calculations of divergence, vertical velocity and vorticity. Bull. Amer. Meteor. Soc., 30, 45-49.

Brown, H. A., 1958: Analysis of a squall line: A line series of mesosystems in different stages of development. Technical Report No. 2, Contract No. 9321, Univ. of Chicago, Dept. of Meteorology.

Brown, H. A., 1962: On the role of the humidity dip in squall line mesosystems. Semi-annual report. USASRDL Contract No. DA 36-039 SC88932, Dept. of Geophysical Sciences, Univ. of Chicago.

Brown, H. A., 1962: The mesoanalysis of an organized convective system. Final report. USASRDL Contract No. DA 36-039 SC88932. Dept. of Geophysical Sciences, Univ. of Chicago.

Byers, H. R., 1942: Nonfrontal thunderstorms. Dept. of Meteorology, Univ. of Chicago Misc. Rep., No. 3, 26 pp.

Byers, H. R., and R. R. Braham, Jr., 1949: The thunderstorm. United States Dept. of Commerce, Washington, D. C.

Fujita, T., 1955: Results of detailed synoptic studies of squall lines. Tellus, 7, 405-436.

Fujita, T., 1957: Three-dimensional mesoanalysis of a squall line. USASEL Contract No. DA 36-039 SC-64656, Meteorological Laboratory, Illinois State Water Survey.

Fujita, T., and H. A. Brown, 1960: Design of a three-dimensional mesometeorological network. Fourth Quarterly Technical Report, USASEL Contract No. DA 36-039 SC-78901, Dept. of Meteorology, Univ. of Chicago.

Fujita, T., H. Newstein and M. Tepper, 1956: Mesoanalysis: An important scale in the analysis of weather data. Res. Paper No. 39, Weather Bureau, Washington, D. C.

Koschmieder, H., 1955: Ergebnisse der Deutschen Boenmessungen. 1939/1941. Flug-meteorologische Forschungsarbeiten, Heft 2.

Newton, C. W., 1950: Structure and mechanism of the prefrontal squall line. J. Meteor., 7, 210-222.

Refsdal, A., 1937: Geofys. Publikasjoner, Norske Videnskaps-Akad. Oslo, Vol. 11.

Stevens, D. W., and J. R. Gerhart, 1959: A new meteorological research tower. Bull. Amer. Meteor. Soc., Vol. 40, No. 1, 24-26.

Suckstorff, G. A., 1935: Die stromungsvorgange in instabilitatschauern. Meteor. Zeit., 52, 449-452.

Tepper, M., et al., 1954: Pressure jump lines in midwestern United States. Research Paper 37, USWB.

Tepper, M., 1957: Mesometeorology: the link between macroscale atmospheric motions and local weather. Presented at IUGG General Assembly, Toronto, 1957.

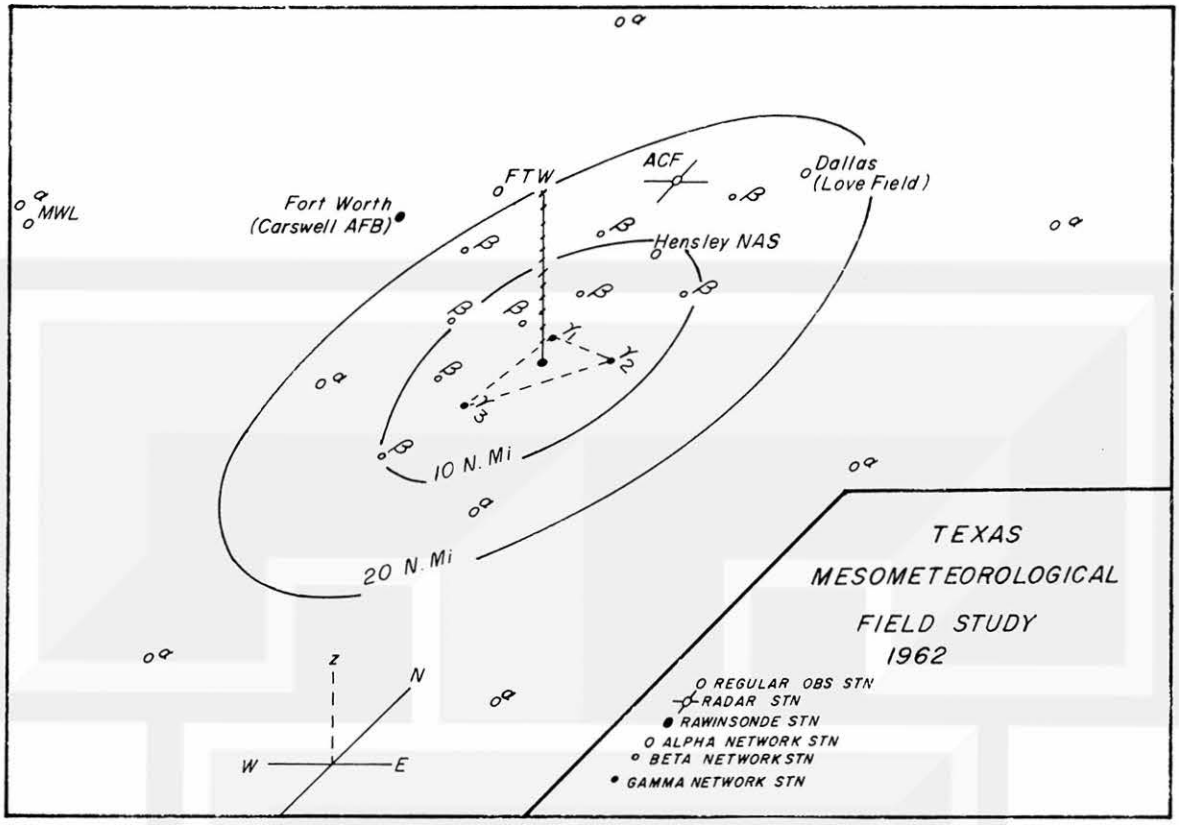

Fig. 1 Network of stations utilized in the 1962 Texas field operation.

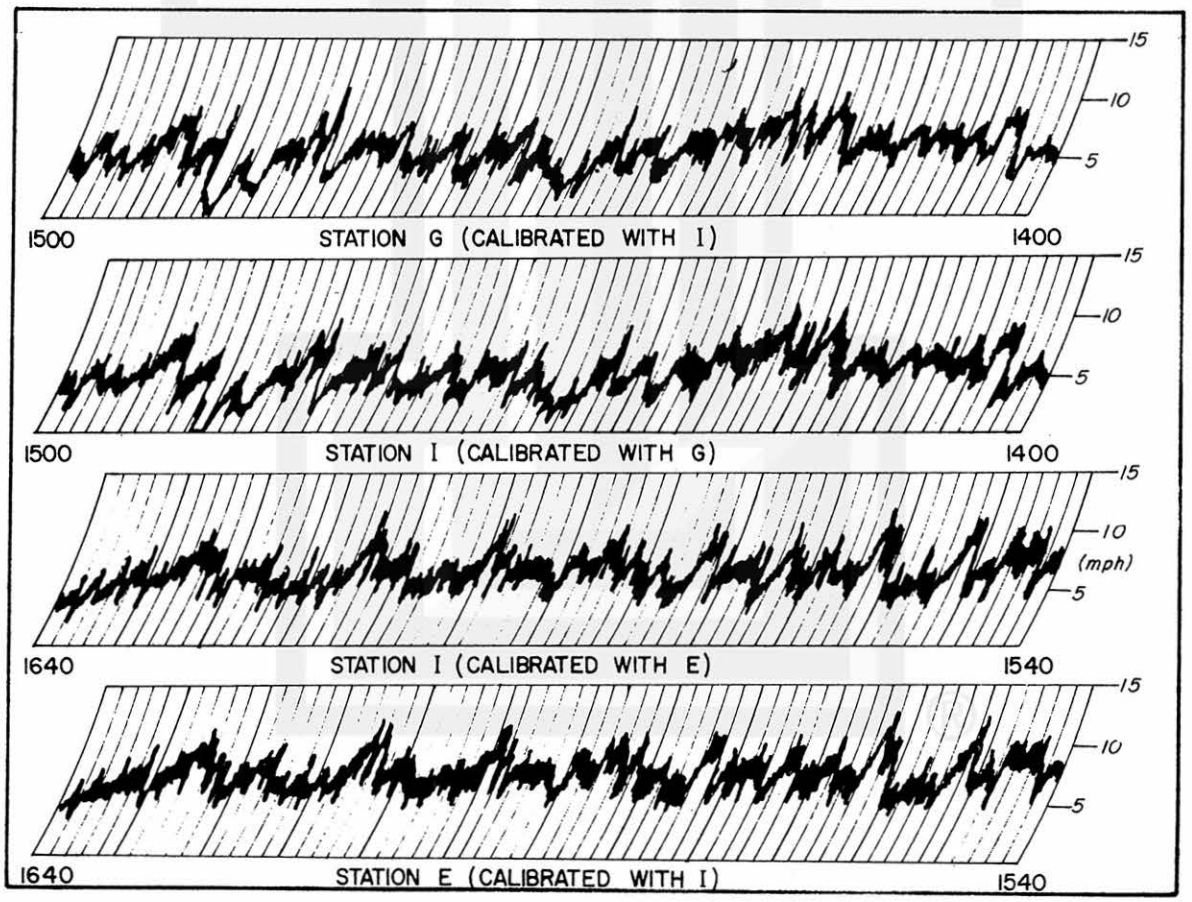

Fig. 2 Comparison of simultaneous wind speed recordings of the Gamma network instruments.

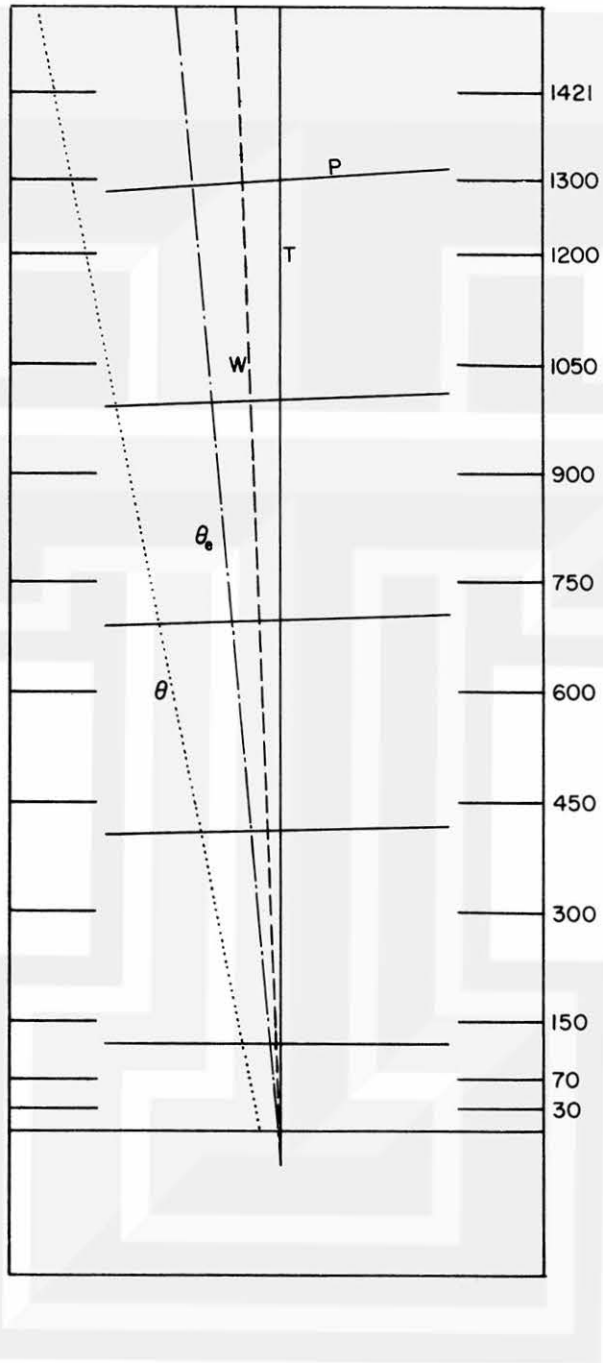

Fig. 3
Overlay

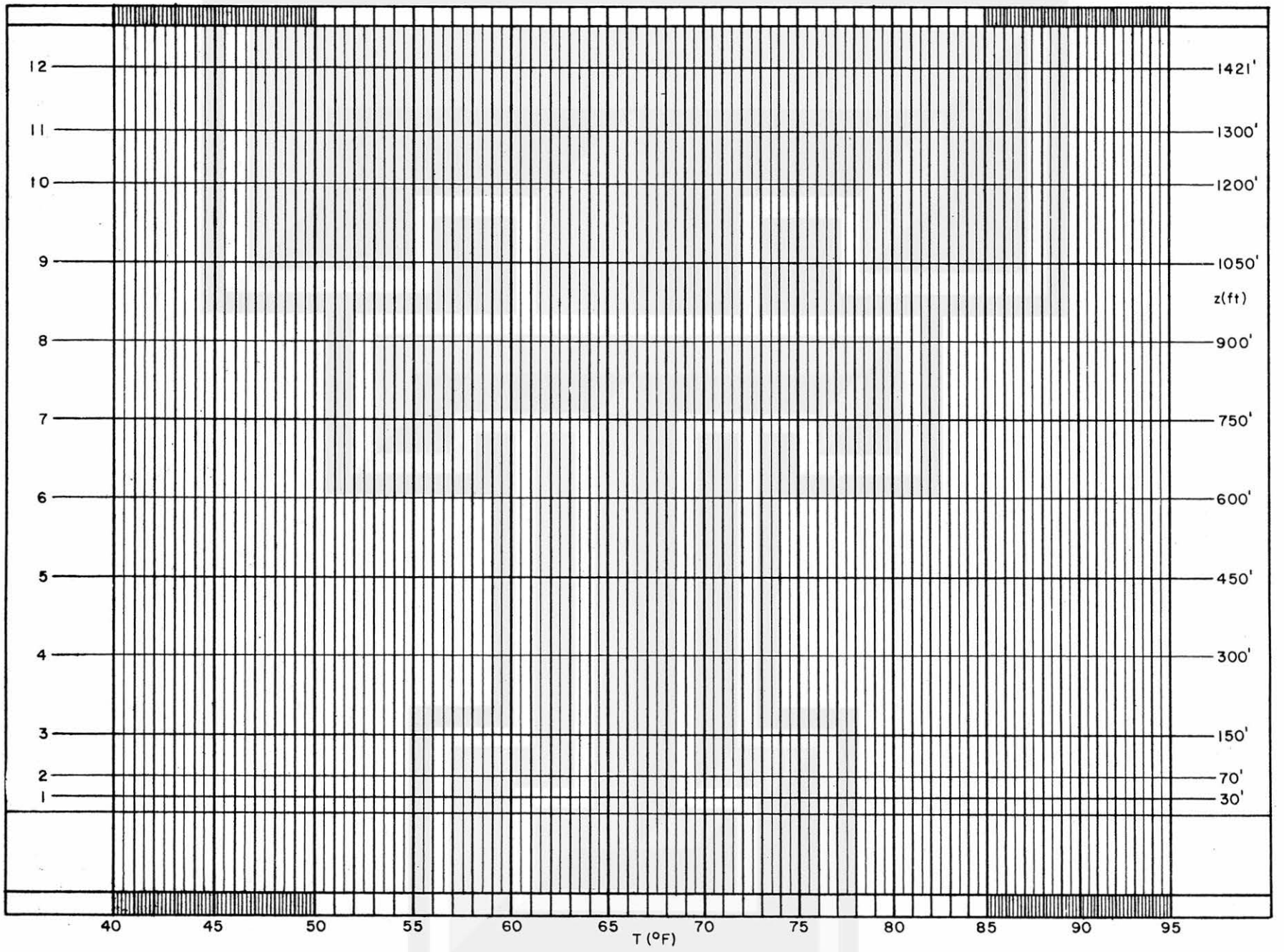

Fig. 3 Low-level thermodynamic diagram containing isolines of temperature (°F), potential temperature (°K), equivalent potential temperature (°K), pressure (mb), and mixing ratio (gm/kg) versus height (ft).

α (DEG) −	α (DEG) +	α (DEG) +	α (DEG) −	SPEED (MPH) 0	2	4	6	8	10	12	14	16	18	20	22	24	26	28	30	32	34	36	38	40
				0	0.4	0.9	1.3	1.8	2.2	2.7	3.1	3.6	4.0	4.4	4.9	5.3	5.8	6.2	6.7	7.1	7.6	8.0	8.4	8.9
335	150	155	330	0	0.4	0.9	1.3	1.8	2.2	2.7	3.1	3.6	4.0	4.4	4.9	5.3	5.8	6.2	6.7	7.1	7.5	8.0	8.4	8.9
				0	0.4	0.9	1.3	1.8	2.2	2.7	3.1	3.5	4.0	4.4	4.9	5.3	5.8	6.2	6.6	7.1	7.5	8.0	8.4	8.9
340	145	160	325	0	0.4	0.9	1.3	1.8	2.2	2.6	3.1	3.5	4.0	4.4	4.8	5.3	5.7	6.2	6.6	7.0	7.5	7.9	8.4	8.8
				0	0.4	0.9	1.3	1.8	2.2	2.6	3.1	3.5	3.9	4.4	4.8	5.3	5.7	6.1	6.6	7.0	7.4	7.9	8.3	8.8
345	140	165	320	0	0.4	0.9	1.3	1.7	2.2	2.6	3.0	3.5	3.9	4.3	4.8	5.2	5.6	6.1	6.5	6.9	7.4	7.8	8.2	8.7
				0	0.4	0.9	1.3	1.7	2.1	2.6	3.0	3.4	3.9	4.3	4.7	5.2	5.6	6.0	6.4	6.9	7.3	7.7	8.2	8.6
350	135	170	315	0	0.4	0.8	1.3	1.7	2.1	2.5	3.0	3.4	3.8	4.2	4.7	5.1	5.5	5.9	6.4	6.8	7.2	7.6	8.1	8.5
				0	0.4	0.8	1.3	1.7	2.1	2.5	2.9	3.3	3.8	4.2	4.6	5.0	5.4	5.8	6.3	6.7	7.1	7.5	7.9	8.4
355	130	175	310	0	0.4	0.8	1.2	1.6	2.1	2.5	2.9	3.3	3.7	4.1	4.5	4.9	5.3	5.7	6.2	6.6	7.0	7.4	7.8	8.2
				0	0.4	0.8	1.2	1.6	2.0	2.4	2.8	3.2	3.6	4.0	4.4	4.8	5.2	5.6	6.0	6.4	6.8	7.3	7.7	8.1
360	125	180	305	0	0.4	0.8	1.2	1.6	2.0	2.4	2.8	3.2	3.5	3.9	4.3	4.7	5.1	5.5	5.9	6.3	6.7	7.1	7.5	7.9
				0	0.4	0.8	1.2	1.5	1.9	2.3	2.7	3.1	3.5	3.9	4.2	4.6	5.0	5.4	5.8	6.2	6.5	6.9	7.3	7.7
5	120	185	300	0	0.4	0.7	1.1	1.5	1.9	2.2	2.6	3.0	3.4	3.8	4.1	4.5	4.9	5.2	5.6	6.0	6.4	6.7	7.1	7.5
				0	0.4	0.7	1.1	1.5	1.8	2.2	2.5	2.9	3.3	3.6	4.0	4.4	4.7	5.1	5.5	5.8	6.2	6.6	6.9	7.3
10	115	190	295	0	0.4	0.7	1.1	1.4	1.8	2.1	2.5	2.8	3.2	3.5	3.9	4.2	4.6	4.9	5.3	5.6	6.0	6.3	6.7	7.1
				0	0.3	0.7	1.0	1.4	1.7	2.0	2.4	2.7	3.1	3.4	3.7	4.1	4.4	4.8	5.1	5.4	5.8	6.1	6.5	6.8
15	110	195	290	0	0.3	0.7	1.0	1.3	1.6	2.0	2.3	2.6	2.9	3.3	3.6	3.9	4.3	4.6	4.9	5.2	5.6	5.9	6.2	6.6
				0	0.3	0.6	0.9	1.3	1.6	1.9	2.2	2.5	2.8	3.1	3.5	3.8	4.1	4.4	4.7	5.0	5.3	5.7	6.0	6.3
20	105	200	285	0	0.3	0.6	0.9	1.2	1.5	1.8	2.1	2.4	2.7	3.0	3.3	3.6	3.9	4.2	4.5	4.8	5.1	5.4	5.7	6.0
				0	0.3	0.6	0.9	1.1	1.4	1.7	2.0	2.3	2.6	2.9	3.1	3.4	3.7	4.0	4.3	4.6	4.9	5.1	5.4	5.7
25	100	205	280	0	0.3	0.5	0.8	1.1	1.4	1.6	1.9	2.2	2.4	2.7	3.0	3.2	3.5	3.8	4.1	4.3	4.6	4.9	5.1	5.4
				0	0.3	0.5	0.8	1.0	1.3	1.5	1.8	2.0	2.3	2.6	2.8	3.1	3.3	3.6	3.8	4.1	4.3	4.6	4.8	5.1
30	95	210	275	0	0.2	0.5	0.7	1.0	1.2	1.4	1.7	1.9	2.1	2.4	2.6	2.9	3.1	3.3	3.6	3.8	4.1	4.3	4.5	4.8
				0	0.2	0.4	0.7	0.9	1.1	1.3	1.6	1.8	2.0	2.2	2.4	2.7	2.9	3.1	3.3	3.6	3.8	4.0	4.2	4.4
35	90	215	270	0	0.2	0.4	0.6	0.8	1.0	1.2	1.4	1.6	1.8	2.1	2.3	2.5	2.7	2.9	3.1	3.3	3.5	3.7	3.9	4.1
				0	0.2	0.4	0.6	0.8	0.9	1.1	1.3	1.5	1.7	1.9	2.1	2.3	2.4	2.6	2.8	3.0	3.2	3.4	3.6	3.8
40	85	220	265	0	0.2	0.3	0.5	0.7	0.9	1.0	1.2	1.4	1.5	1.7	1.9	2.0	2.2	2.4	2.6	2.7	2.9	3.1	3.2	3.4
				0	0.2	0.3	0.5	0.6	0.8	0.9	1.1	1.2	1.4	1.5	1.7	1.8	2.0	2.1	2.3	2.4	2.6	2.7	2.9	3.0
45	80	225	260	0	0.1	0.3	0.4	0.5	0.7	0.8	0.9	1.1	1.2	1.3	1.5	1.6	1.7	1.9	2.0	2.1	2.3	2.4	2.5	2.7
				0	0.1	0.2	0.3	0.5	0.6	0.7	0.8	0.9	1.0	1.2	1.3	1.4	1.5	1.6	1.7	1.8	2.0	2.1	2.2	2.3
50	75	230	255	0	0.1	0.2	0.3	0.4	0.5	0.6	0.7	0.8	0.9	1.0	1.1	1.2	1.3	1.3	1.4	1.5	1.6	1.7	1.8	1.9
				0	0.1	0.2	0.2	0.3	0.4	0.5	0.5	0.6	0.7	0.8	0.8	0.9	1.0	1.1	1.2	1.2	1.3	1.4	1.5	1.5
55	70	235	250	0	0.1	0.1	0.2	0.2	0.3	0.3	0.4	0.5	0.5	0.6	0.6	0.7	0.8	0.8	0.9	0.9	1.0	1.0	1.1	1.2
				0	0	0.1	0.1	0.2	0.2	0.2	0.3	0.3	0.3	0.4	0.4	0.5	0.5	0.5	0.6	0.6	0.7	0.7	0.7	0.8
60	65	240	245	0	0	0	0.1	0.1	0.1	0.1	0.1	0.2	0.2	0.2	0.2	0.2	0.3	0.3	0.3	0.3	0.3	0.3	0.4	0.4
				0	0	0	0	0	0	0	0	0	0	0	0	0	0	0	0	0	0	0	0	0

STATION G - γ_1

Fig. 4 Divergence (and vorticity) computation table for Station G.

α (DEG) +	α (DEG) −	α (DEG) −	α (DEG) +	SPEED (MPH) 0	2	4	6	8	10	12	14	16	18	20	22	24	26	28	30	32	34	36	38	40
290	110	110	290	0	0.3	0.6	0.9	1.2	1.5	1.8	2.2	2.5	2.8	3.1	3.4	3.7	4.0	4.3	4.6	4.9	5.2	5.5	5.8	6.2
				0	0.3	0.6	0.9	1.2	1.5	1.8	2.2	2.5	2.8	3.1	3.4	3.7	4.0	4.3	4.6	4.9	5.2	5.5	5.8	6.1
295	105	115	285	0	0.3	0.6	0.9	1.2	1.5	1.8	2.1	2.5	2.8	3.1	3.4	3.7	4.0	4.3	4.6	4.9	5.2	5.5	5.8	6.1
				0	0.3	0.6	0.9	1.2	1.5	1.8	2.1	2.4	2.7	3.1	3.4	3.7	4.0	4.3	4.6	4.9	5.2	5.5	5.8	6.1
300	100	120	280	0	0.3	0.6	0.9	1.2	1.5	1.8	2.1	2.4	2.7	3.0	3.3	3.6	3.9	4.2	4.5	4.8	5.2	5.5	5.8	6.1
				0	0.3	0.6	0.9	1.2	1.5	1.8	2.1	2.4	2.7	3.0	3.3	3.6	3.9	4.2	4.5	4.8	5.1	5.4	5.7	6.0
305	95	125	275	0	0.3	0.6	0.9	1.2	1.5	1.8	2.1	2.4	2.7	3.0	3.3	3.6	3.9	4.2	4.5	4.8	5.1	5.3	5.6	5.9
				0	0.3	0.6	0.9	1.2	1.5	1.8	2.1	2.3	2.6	2.9	3.2	3.5	3.8	4.1	4.4	4.7	5.0	5.3	5.6	5.9
310	90	130	270	0	0.3	0.6	0.9	1.2	1.4	1.7	2.0	2.3	2.6	2.9	3.2	3.5	3.8	4.0	4.3	4.6	4.9	5.2	5.5	5.8
				0	0.3	0.6	0.9	1.1	1.4	1.7	2.0	2.3	2.6	2.8	3.1	3.4	3.7	4.0	4.3	4.5	4.8	5.1	5.4	5.7
315	85	135	265	0	0.3	0.6	0.8	1.1	1.4	1.7	2.0	2.2	2.5	2.8	3.1	3.3	3.6	3.9	4.2	4.5	4.7	5.0	5.3	5.6
				0	0.3	0.5	0.8	1.1	1.4	1.6	1.9	2.2	2.5	2.7	3.0	3.3	3.5	3.8	4.1	4.4	4.6	4.9	5.2	5.5
320	80	140	260	0	0.3	0.5	0.8	1.1	1.3	1.6	1.9	2.1	2.4	2.7	2.9	3.2	3.5	3.7	4.0	4.3	4.5	4.8	5.1	5.3
				0	0.3	0.5	0.8	1.0	1.3	1.6	1.8	2.1	2.3	2.6	2.9	3.1	3.4	3.6	3.9	4.2	4.4	4.7	4.9	5.2
325	75	145	255	0	0.3	0.5	0.8	1.0	1.3	1.5	1.8	2.0	2.3	2.5	2.8	3.0	3.3	3.5	3.8	4.0	4.3	4.5	4.8	5.0
				0	0.2	0.5	0.7	1.0	1.2	1.5	1.7	2.0	2.2	2.4	2.7	2.9	3.2	3.4	3.7	3.9	4.2	4.4	4.6	4.9
330	70	150	250	0	0.2	0.5	0.7	0.9	1.2	1.4	1.7	1.9	2.1	2.4	2.6	2.8	3.1	3.3	3.5	3.8	4.0	4.2	4.5	4.7
				0	0.2	0.5	0.7	0.9	1.1	1.4	1.6	1.8	2.0	2.3	2.5	2.7	2.9	3.2	3.4	3.6	3.9	4.1	4.3	4.5
335	65	155	245	0	0.2	0.4	0.7	0.9	1.1	1.3	1.5	1.7	2.0	2.2	2.4	2.6	2.8	3.0	3.3	3.5	3.7	3.9	4.1	4.4
				0	0.2	0.4	0.6	0.8	1.0	1.2	1.5	1.7	1.9	2.1	2.3	2.5	2.7	2.9	3.1	3.3	3.5	3.7	3.9	4.2
340	60	160	240	0	0.2	0.4	0.6	0.8	1.0	1.2	1.4	1.6	1.8	2.0	2.2	2.4	2.6	2.8	3.0	3.2	3.4	3.6	3.8	4.0
				0	0.2	0.4	0.6	0.7	0.9	1.1	1.3	1.5	1.7	1.9	2.1	2.2	2.4	2.6	2.8	3.0	3.2	3.4	3.6	3.7
345	55	165	235	0	0.2	0.4	0.5	0.7	0.9	1.1	1.2	1.4	1.6	1.8	1.9	2.1	2.3	2.5	2.6	2.8	3.0	3.2	3.4	3.5
				0	0.2	0.3	0.5	0.7	0.8	1.0	1.2	1.3	1.5	1.7	1.8	2.0	2.2	2.3	2.5	2.6	2.8	3.0	3.1	3.3
350	50	170	230	0	0.2	0.3	0.5	0.6	0.8	0.9	1.1	1.2	1.4	1.5	1.7	1.8	2.0	2.2	2.3	2.5	2.6	2.8	2.9	3.1
				0	0.1	0.3	0.4	0.6	0.7	0.8	1.0	1.1	1.3	1.4	1.6	1.7	1.8	2.0	2.1	2.3	2.4	2.6	2.7	2.8
355	45	175	225	0	0.1	0.3	0.4	0.5	0.7	0.8	0.9	1.0	1.2	1.3	1.4	1.6	1.7	1.8	2.0	2.1	2.2	2.3	2.5	2.6
				0	0.1	0.2	0.4	0.5	0.6	0.7	0.8	0.9	1.1	1.2	1.3	1.4	1.5	1.6	1.8	1.9	2.0	2.1	2.2	2.4
360	40	180	220	0	0.1	0.2	0.3	0.4	0.5	0.6	0.7	0.8	0.9	1.1	1.2	1.3	1.4	1.5	1.6	1.7	1.8	1.9	2.0	2.1
				0	0.1	0.2	0.3	0.4	0.5	0.6	0.6	0.7	0.8	0.9	1.0	1.1	1.2	1.3	1.4	1.5	1.6	1.7	1.8	1.9
5	35	185	215	0	0.1	0.2	0.2	0.3	0.4	0.5	0.6	0.6	0.7	0.8	0.9	1.0	1.0	1.1	1.2	1.3	1.4	1.4	1.5	1.6
				0	0.1	0.1	0.2	0.3	0.3	0.4	0.5	0.5	0.6	0.7	0.7	0.8	0.9	0.9	1.0	1.1	1.1	1.2	1.3	1.3
10	30	190	210	0	0.1	0.1	0.2	0.2	0.3	0.3	0.4	0.4	0.5	0.5	0.6	0.6	0.7	0.7	0.8	0.9	0.9	1.0	1.0	1.1
				0	0	0.1	0.1	0.2	0.2	0.2	0.3	0.3	0.4	0.4	0.4	0.5	0.5	0.6	0.6	0.6	0.7	0.7	0.8	0.8
15	25	195	205	0	0	0.1	0.1	0.1	0.1	0.2	0.2	0.2	0.2	0.3	0.3	0.3	0.3	0.4	0.4	0.4	0.5	0.5	0.5	0.5
				0	0	0	0	0.1	0.1	0.1	0.1	0.1	0.1	0.1	0.1	0.2	0.2	0.2	0.2	0.2	0.2	0.2	0.3	0.3
20	20	200	200	0	0	0	0	0	0	0	0	0	0	0	0	0	0	0	0	0	0	0	0	0

STATION I – γ_2

Fig. 5 Divergence (and vorticity) computation table for Station I.

α (DEG) +	−	−	+	SPEED (MPH) 0	2	4	6	8	10	12	14	16	18	20	22	24	26	28	30	32	34	36	38	40
15	195	195	15	0	0.3	0.6	0.9	1.2	1.5	1.8	2.2	2.5	2.8	3.1	3.4	3.7	4.0	4.3	4.6	4.9	5.2	5.5	5.8	6.2
				0	0.3	0.6	0.9	1.2	1.5	1.8	2.2	2.5	2.8	3.1	3.4	3.7	4.0	4.3	4.6	4.9	5.2	5.5	5.8	6.1
20	190	200	10	0	0.3	0.6	0.9	1.2	1.5	1.8	2.1	2.5	2.8	3.1	3.4	3.7	4.0	4.3	4.6	4.9	5.2	5.5	5.8	6.1
				0	0.3	0.6	0.9	1.2	1.5	1.8	2.1	2.4	2.7	3.1	3.4	3.7	4.0	4.3	4.6	4.9	5.2	5.5	5.8	6.1
25	185	205	5	0	0.3	0.6	0.9	1.2	1.5	1.8	2.1	2.4	2.7	3.0	3.3	3.6	3.9	4.2	4.5	4.8	5.2	5.5	5.8	6.1
				0	0.3	0.6	0.9	1.2	1.5	1.8	2.1	2.4	2.7	3.0	3.3	3.6	3.9	4.2	4.5	4.8	5.1	5.4	5.7	6.0
30	180	210	360	0	0.3	0.6	0.9	1.2	1.5	1.8	2.1	2.4	2.7	3.0	3.3	3.6	3.9	4.2	4.5	4.8	5.1	5.3	5.6	5.9
				0	0.3	0.6	0.9	1.2	1.5	1.8	2.1	2.3	2.6	2.9	3.2	3.5	3.8	4.1	4.4	4.7	5.0	5.3	5.6	5.9
35	175	215	355	0	0.3	0.6	0.9	1.2	1.4	1.7	2.0	2.3	2.6	2.9	3.2	3.5	3.8	4.0	4.3	4.6	4.9	5.2	5.5	5.8
				0	0.3	0.6	0.9	1.1	1.4	1.7	2.0	2.3	2.6	2.8	3.1	3.4	3.7	4.0	4.3	4.5	4.8	5.1	5.4	5.7
40	170	220	350	0	0.3	0.6	0.8	1.1	1.4	1.7	2.0	2.2	2.5	2.8	3.1	3.3	3.6	3.9	4.2	4.5	4.7	5.0	5.3	5.6
				0	0.3	0.5	0.8	1.1	1.4	1.6	1.9	2.2	2.5	2.7	3.0	3.3	3.5	3.8	4.1	4.4	4.6	4.9	5.2	5.5
45	165	225	345	0	0.3	0.5	0.8	1.1	1.3	1.6	1.9	2.1	2.4	2.7	2.9	3.2	3.5	3.7	4.0	4.3	4.5	4.8	5.1	5.3
				0	0.3	0.5	0.8	1.0	1.3	1.6	1.8	2.1	2.3	2.6	2.9	3.1	3.4	3.6	3.9	4.2	4.4	4.7	4.9	5.2
50	160	230	340	0	0.3	0.5	0.8	1.0	1.3	1.5	1.8	2.0	2.3	2.5	2.8	3.0	3.3	3.5	3.8	4.0	4.3	4.5	4.8	5.0
				0	0.2	0.5	0.7	1.0	1.2	1.5	1.7	2.0	2.2	2.4	2.7	2.9	3.2	3.4	3.7	3.9	4.2	4.4	4.6	4.9
55	155	235	335	0	0.2	0.5	0.7	0.9	1.2	1.4	1.7	1.9	2.1	2.4	2.6	2.8	3.1	3.3	3.5	3.8	4.0	4.2	4.5	4.7
				0	0.2	0.5	0.7	0.9	1.1	1.4	1.6	1.8	2.0	2.3	2.5	2.7	2.9	3.2	3.4	3.6	3.9	4.1	4.3	4.5
60	150	240	330	0	0.2	0.4	0.7	0.9	1.1	1.3	1.5	1.7	2.0	2.2	2.4	2.6	2.8	3.0	3.3	3.5	3.7	3.9	4.1	4.4
				0	0.2	0.4	0.6	0.8	1.0	1.2	1.5	1.7	1.9	2.1	2.3	2.5	2.7	2.9	3.1	3.3	3.5	3.7	3.9	4.2
65	145	245	325	0	0.2	0.4	0.6	0.8	1.0	1.2	1.4	1.6	1.8	2.0	2.2	2.4	2.6	2.8	3.0	3.2	3.4	3.6	3.8	4.0
				0	0.2	0.4	0.6	0.7	0.9	1.1	1.3	1.5	1.7	1.9	2.1	2.2	2.4	2.6	2.8	3.0	3.2	3.4	3.6	3.7
70	140	250	320	0	0.2	0.4	0.5	0.7	0.9	1.1	1.2	1.4	1.6	1.8	1.9	2.1	2.3	2.5	2.6	2.8	3.0	3.2	3.4	3.5
				0	0.2	0.3	0.5	0.7	0.8	1.0	1.2	1.3	1.5	1.7	1.8	2.0	2.2	2.3	2.5	2.6	2.8	3.0	3.1	3.3
75	135	255	315	0	0.2	0.3	0.5	0.6	0.8	0.9	1.1	1.2	1.4	1.5	1.7	1.8	2.0	2.2	2.3	2.5	2.6	2.8	2.9	3.1
				0	0.1	0.3	0.4	0.6	0.7	0.8	1.0	1.1	1.3	1.4	1.6	1.7	1.8	2.0	2.1	2.3	2.4	2.6	2.7	2.8
80	130	260	310	0	0.1	0.3	0.4	0.5	0.7	0.8	0.9	1.0	1.2	1.3	1.4	1.6	1.7	1.8	2.0	2.1	2.2	2.3	2.5	2.6
				0	0.1	0.2	0.4	0.5	0.6	0.7	0.8	0.9	1.1	1.2	1.3	1.4	1.5	1.6	1.8	1.9	2.0	2.1	2.2	2.4
85	125	265	305	0	0.1	0.2	0.3	0.4	0.5	0.6	0.7	0.8	0.9	1.1	1.2	1.3	1.4	1.5	1.6	1.7	1.8	1.9	2.0	2.1
				0	0.1	0.2	0.3	0.4	0.5	0.6	0.6	0.7	0.8	0.9	1.0	1.1	1.2	1.3	1.4	1.5	1.6	1.7	1.8	1.9
90	120	270	300	0	0.1	0.2	0.2	0.3	0.4	0.5	0.6	0.6	0.7	0.8	0.9	1.0	1.0	1.1	1.2	1.3	1.4	1.4	1.5	1.6
				0	0.1	0.1	0.2	0.3	0.3	0.4	0.5	0.5	0.6	0.7	0.7	0.8	0.9	0.9	1.0	1.1	1.1	1.2	1.3	1.3
95	115	275	295	0	0.1	0.1	0.2	0.2	0.3	0.3	0.4	0.4	0.5	0.5	0.6	0.6	0.7	0.7	0.8	0.9	0.9	1.0	1.0	1.1
				0	0	0.1	0.1	0.2	0.2	0.2	0.3	0.3	0.4	0.4	0.4	0.5	0.5	0.6	0.6	0.6	0.7	0.7	0.8	0.8
100	110	280	290	0	0	0.1	0.1	0.1	0.1	0.2	0.2	0.2	0.2	0.3	0.3	0.3	0.3	0.4	0.4	0.4	0.5	0.5	0.5	0.5
				0	0	0	0	0.1	0.1	0.1	0.1	0.1	0.1	0.1	0.1	0.2	0.2	0.2	0.2	0.2	0.2	0.2	0.3	0.3
105	105	285	285	0	0	0	0	0	0	0	0	0	0	0	0	0	0	0	0	0	0	0	0	0

STATION E − γ_3

Fig. 6 Divergence (and vorticity) computation table for Station E.

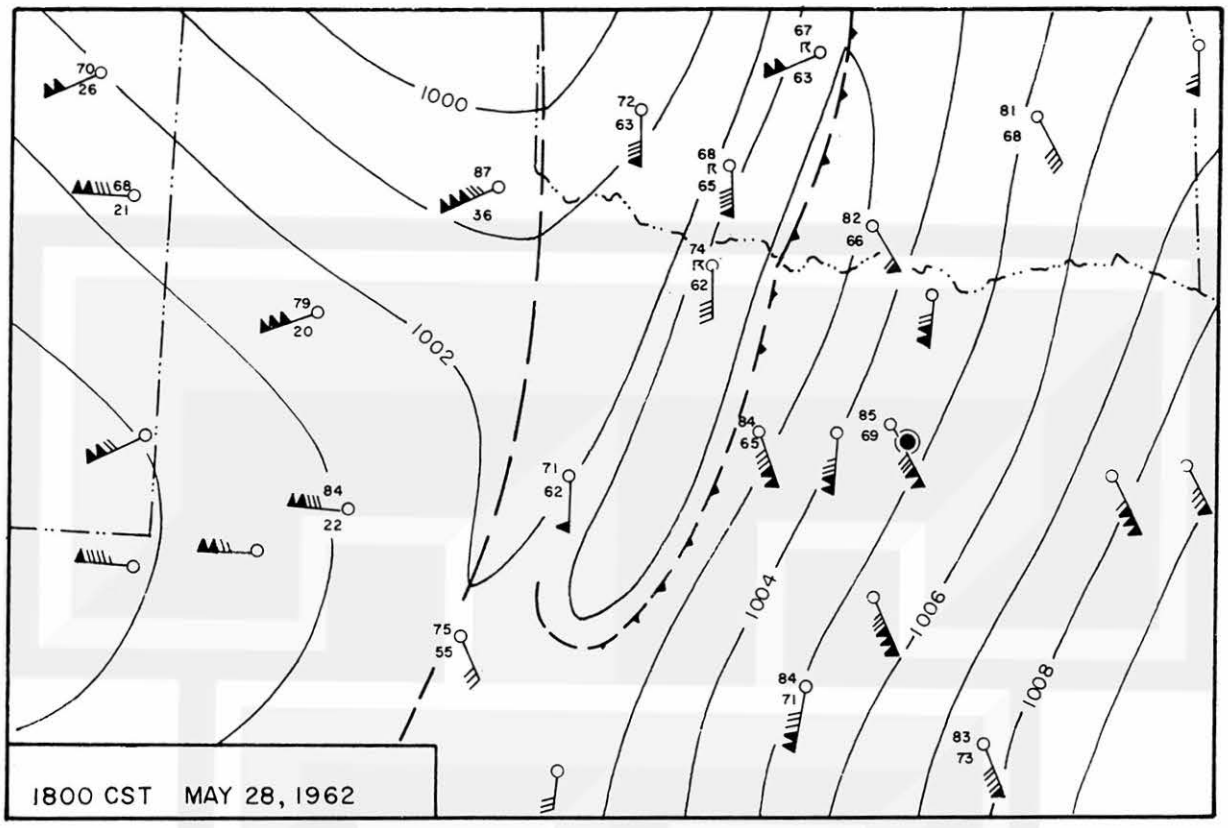

Fig. 7 Surface synoptic chart. Mesonetwork area is indicated by solid circle. Pressure (1-mb intervals) and wind (1 barb = 2 mph, 1 pennant = 10 mph) are also noted.

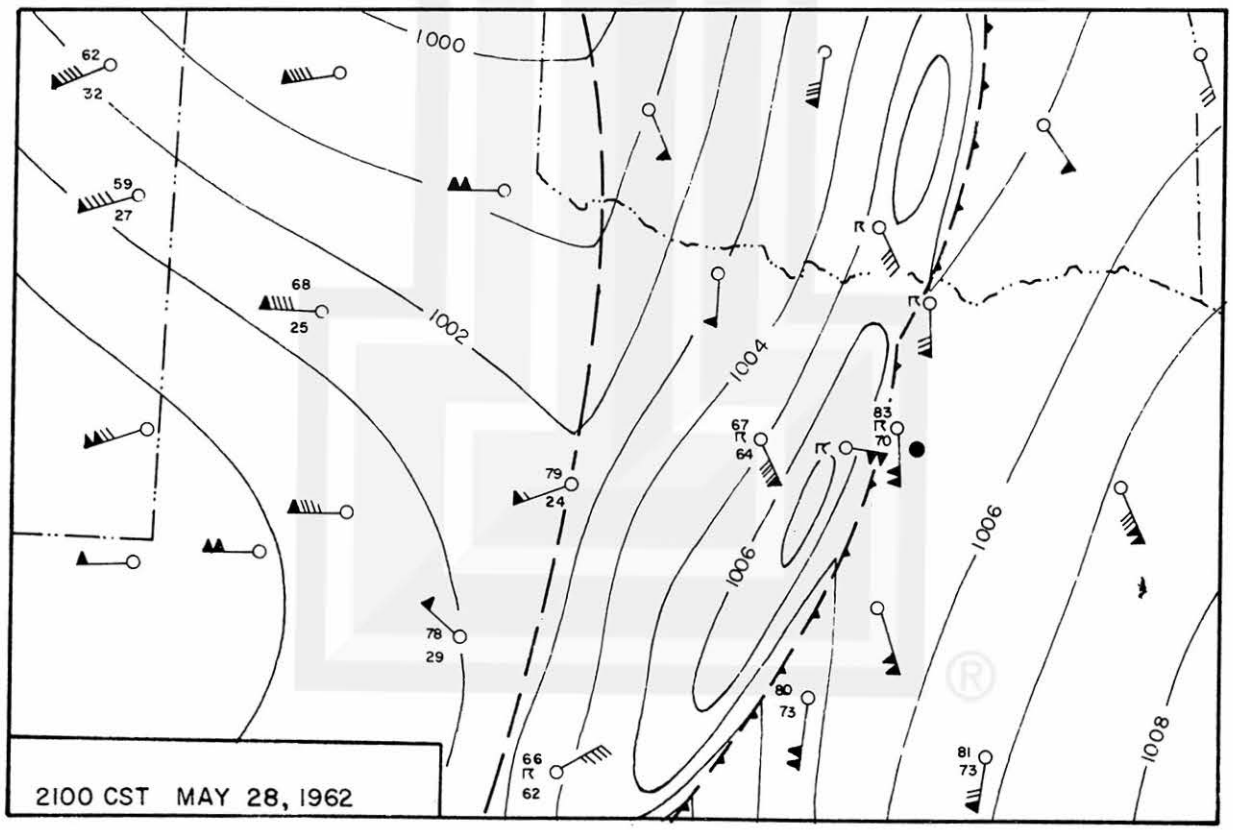

Fig. 8 Surface synoptic chart.

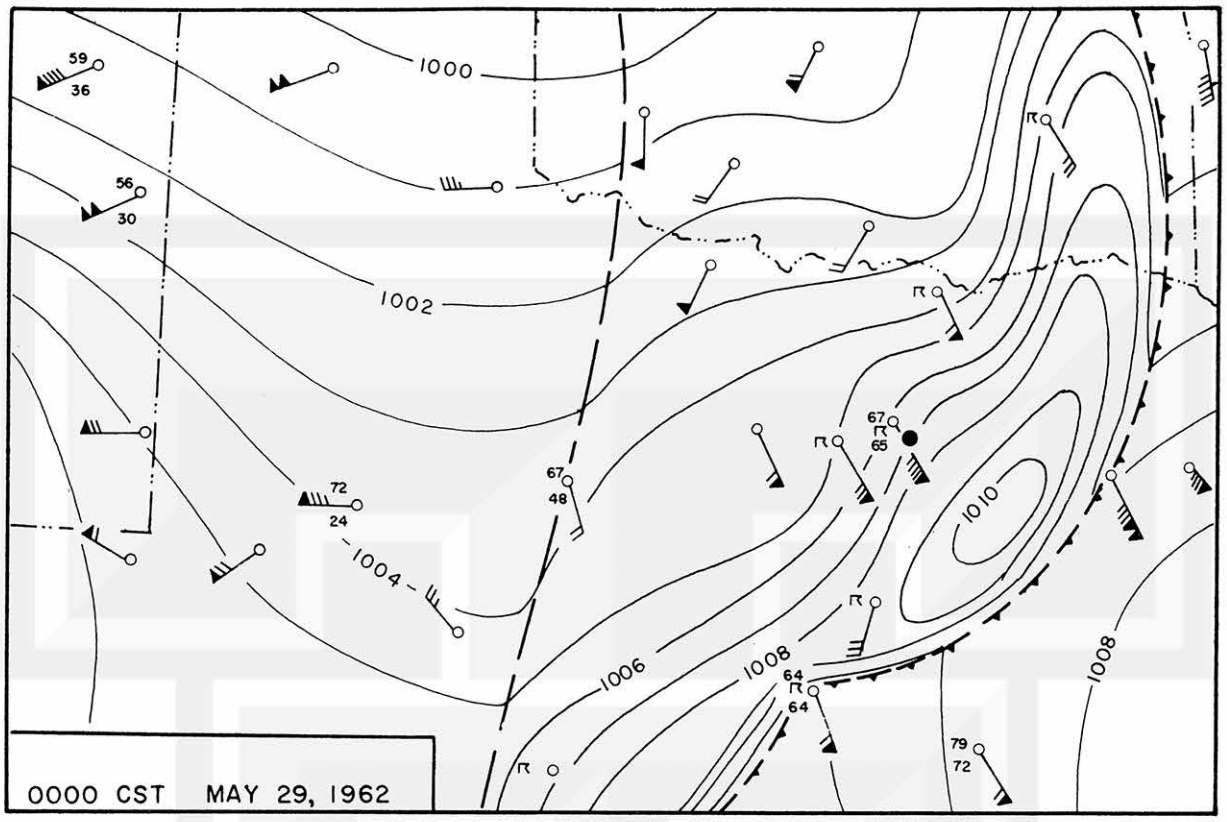

Fig. 9 Surface synoptic chart.

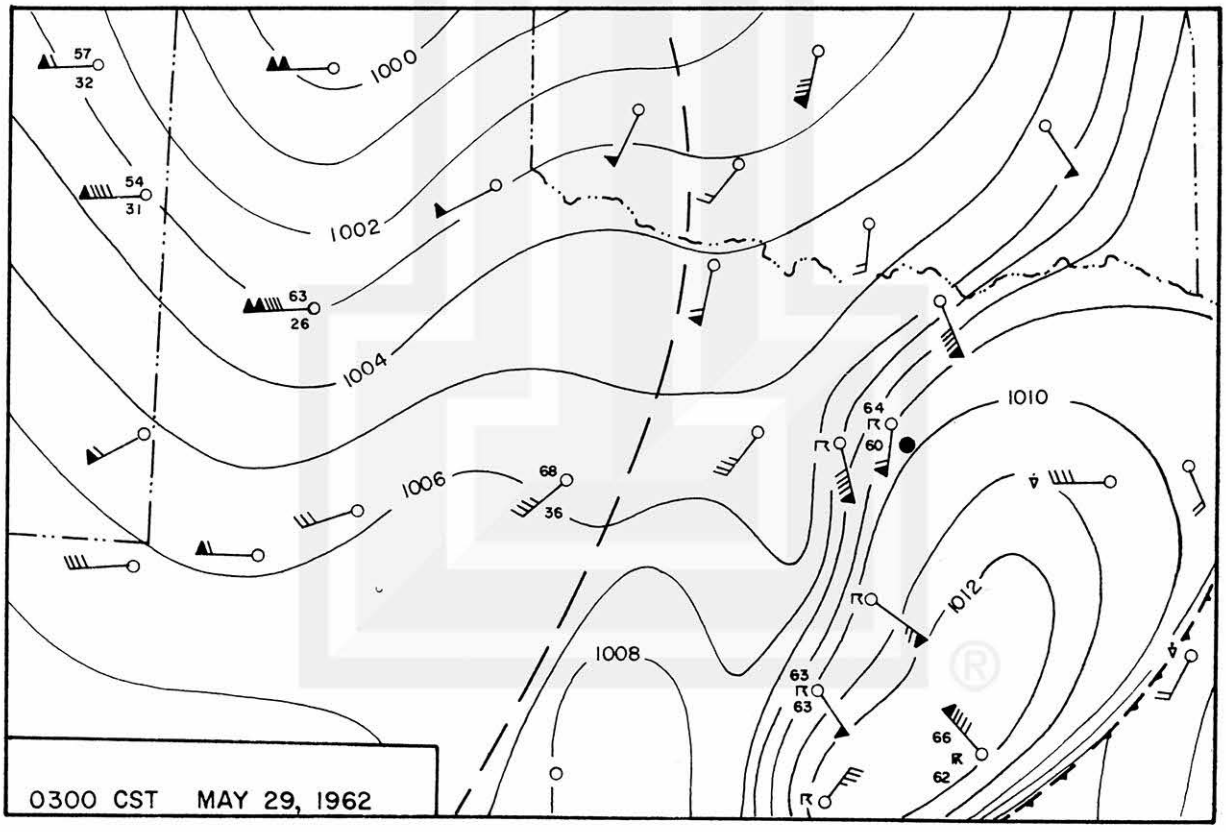

Fig. 10 Surface synoptic chart.

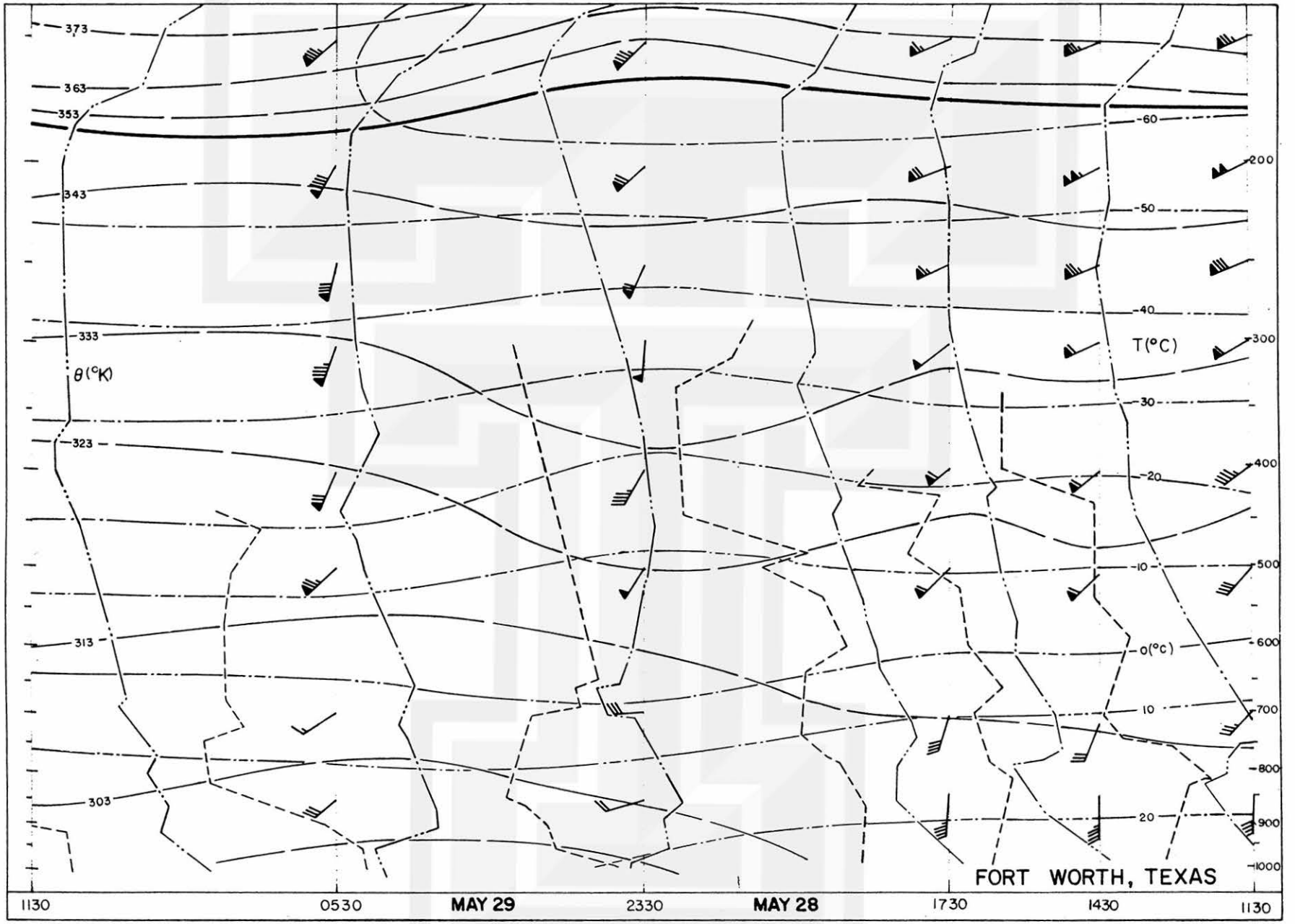

Fig. 11 Time cross-section of wind (1 pennant = 50 knots), temperature (°C, dash-dot line), and potential temperature (°K, dash line) at Fort Worth. Vertical soundings of temperature and dew point are also shown.

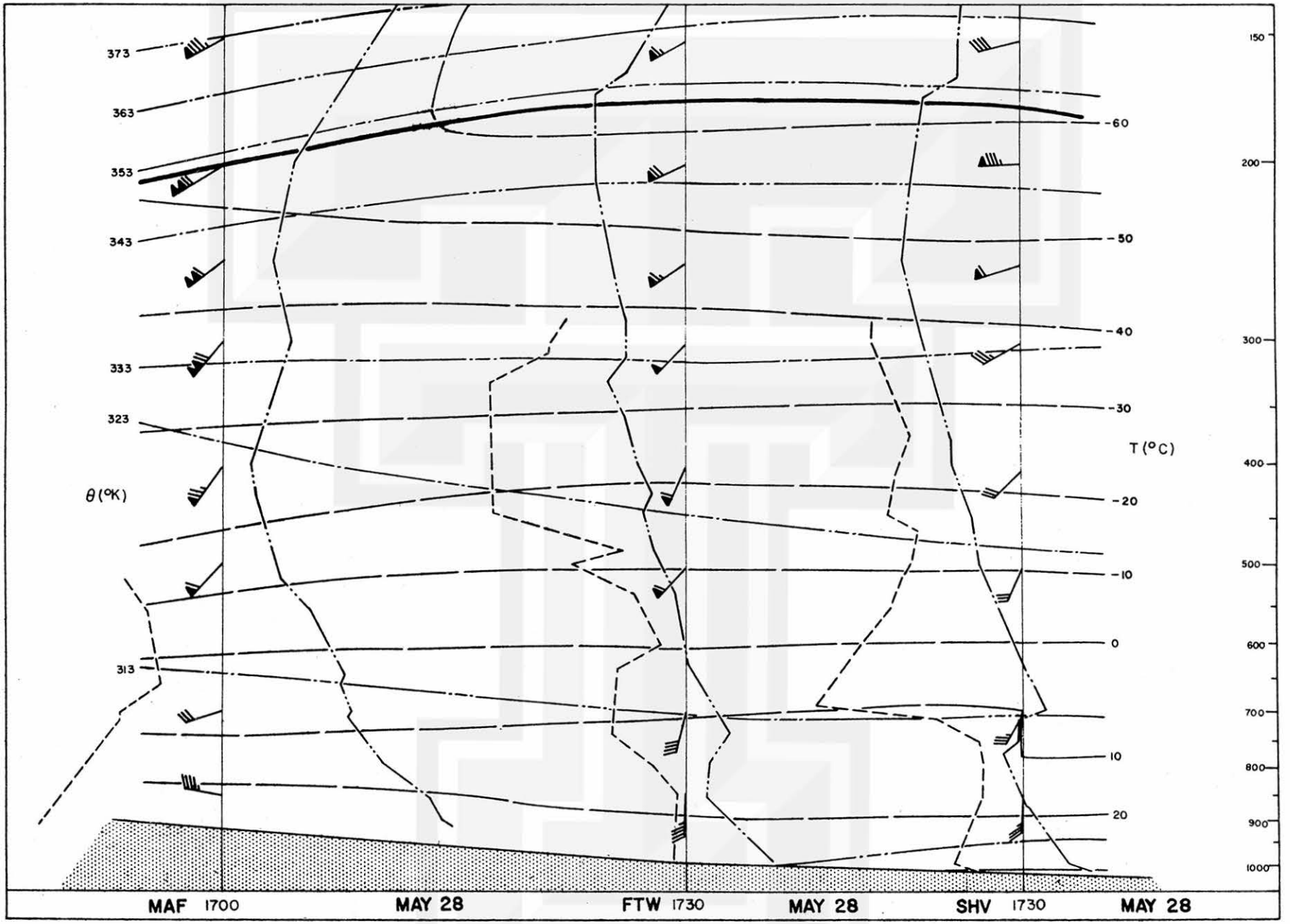

Fig. 12 Space cross-section between Midland, Texas, and Shreveport, La. Isolines same as in Fig. 11.

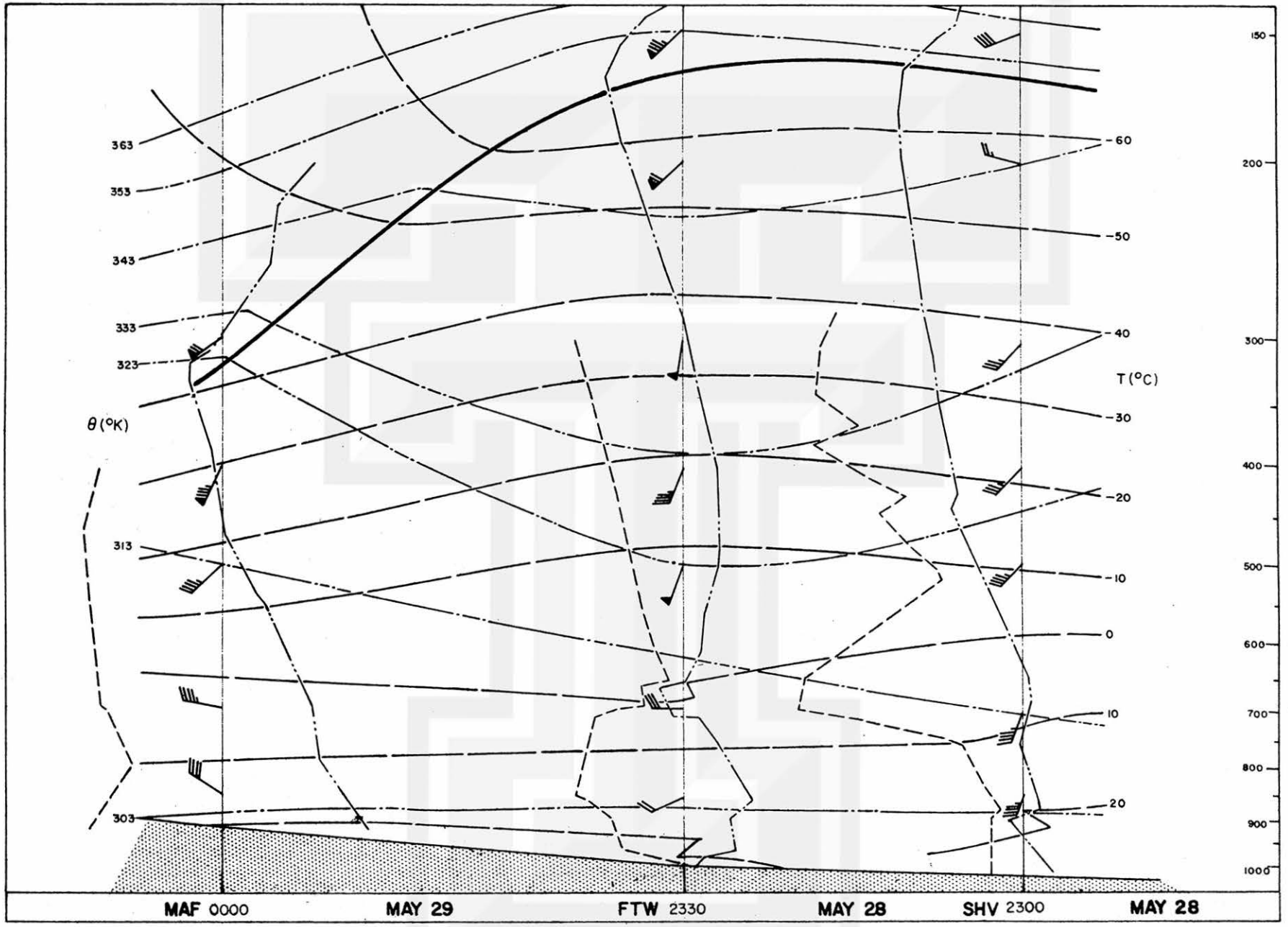

Fig. 13 Space cross-section between Midland, Texas, and Shreveport, La. Isolines same as in Fig. 11.

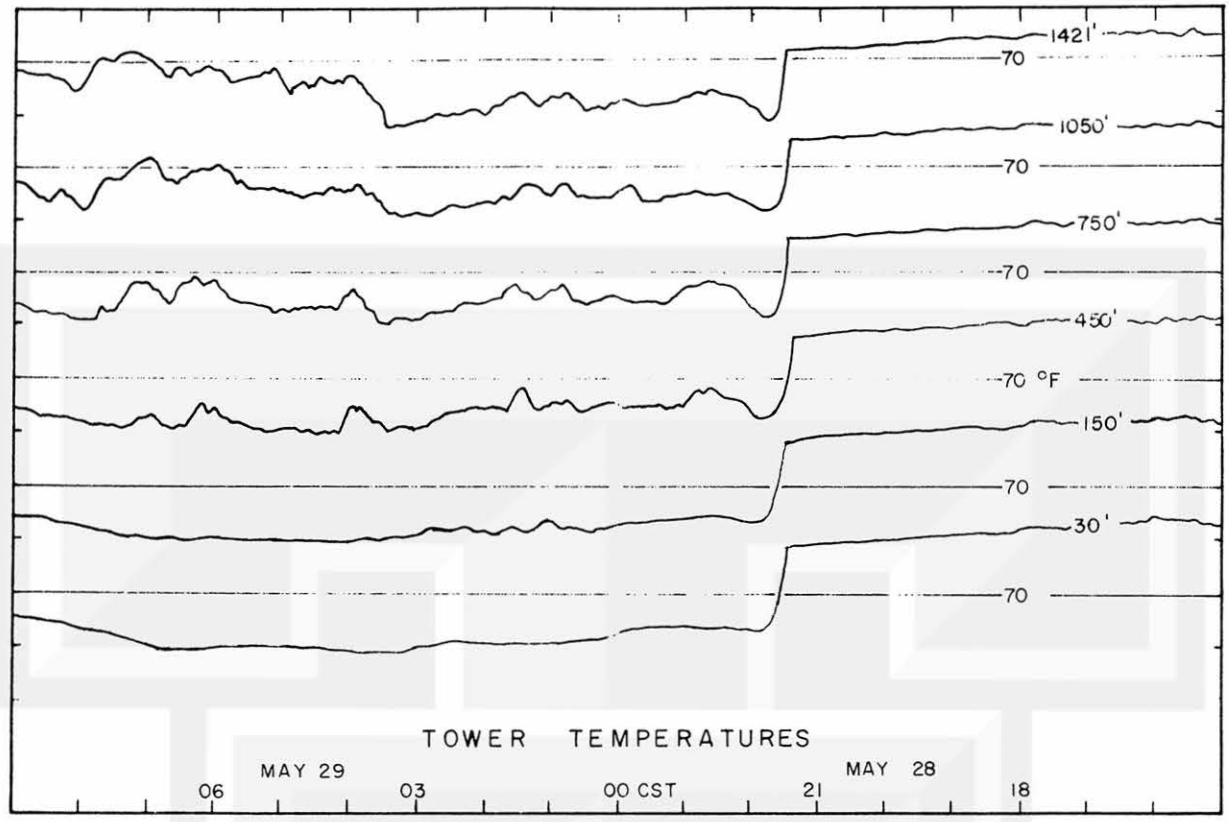

Fig. 14a Time sections of temperatures as recorded by six hygrothermographs placed at selected levels on television tower.

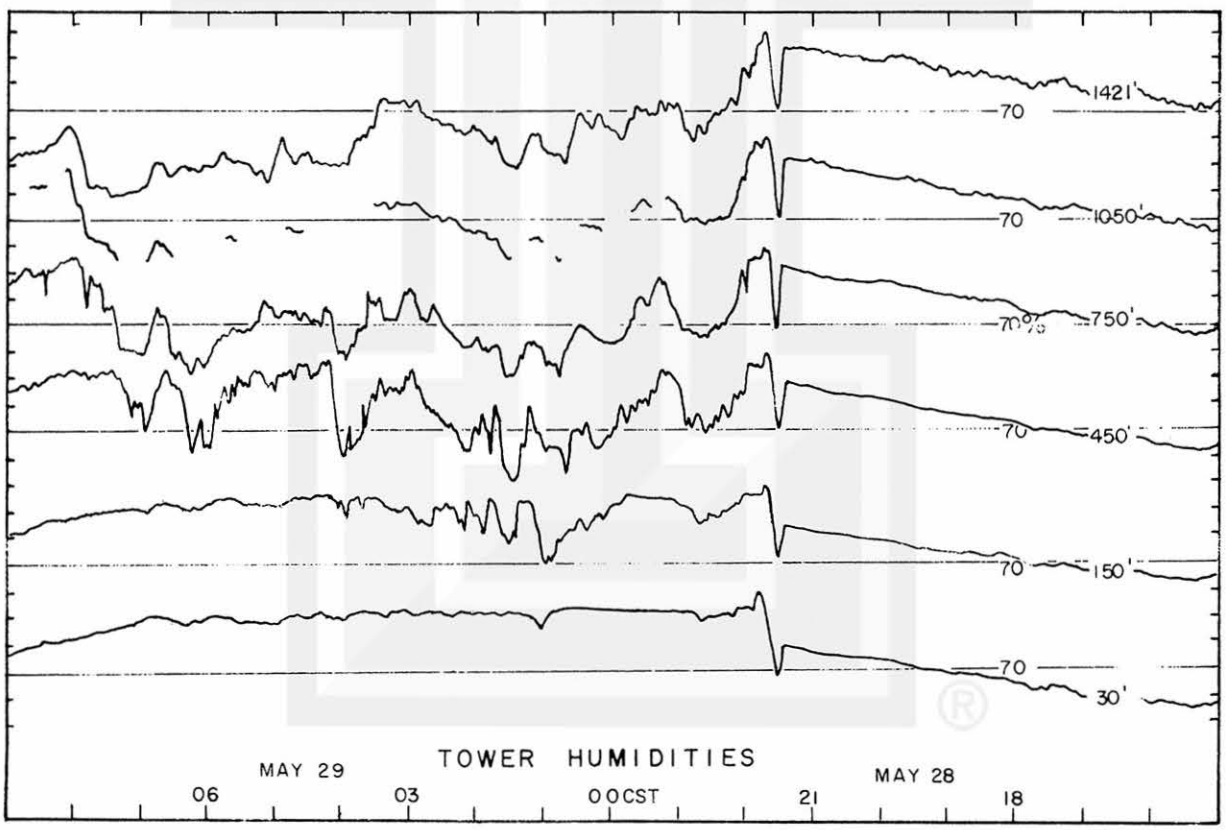

Fig. 14b Time sections of relative humidity as recorded by six hygrothermographs placed at selected levels on television tower.

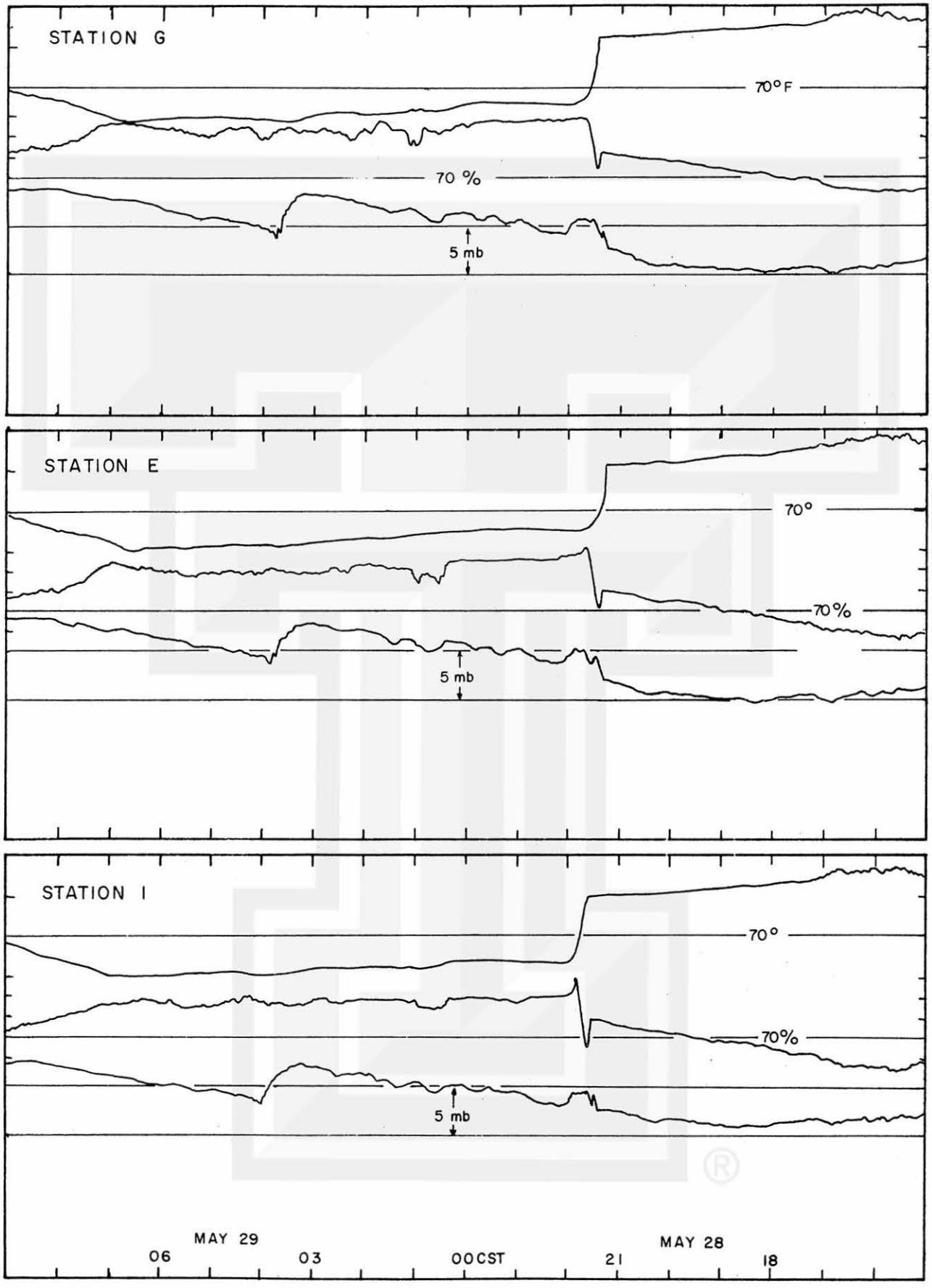

Fig. 15 Time sections of temperature, relative humidity and pressure from Gamma network stations.

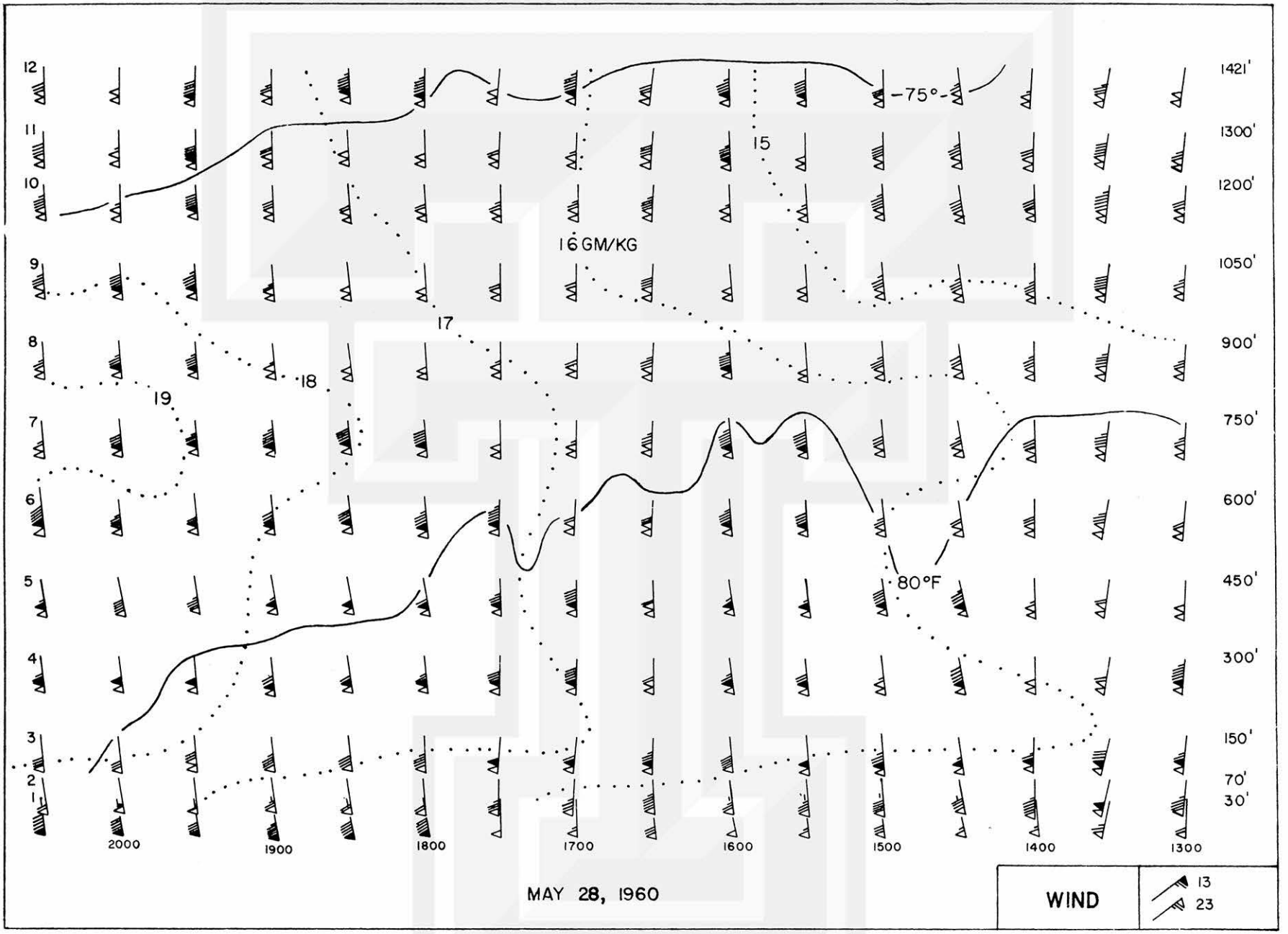

Fig. 16 Time variation of temperature (°F), mixing ratio (gm/kg), and wind (mph) in the lower layers of a pre-squall line environment.

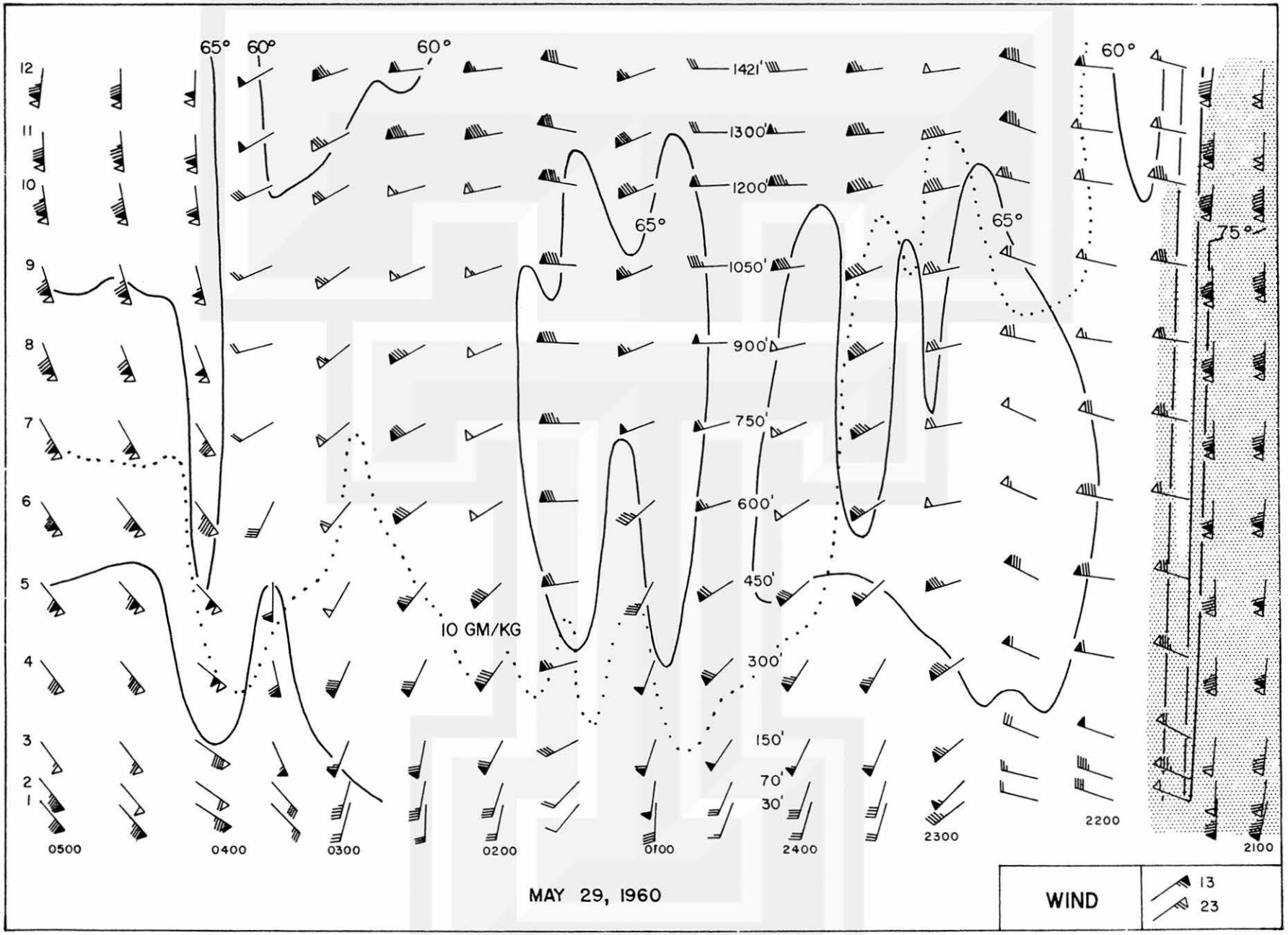

Fig. 17 Time variation of temperature (°F), mixing ratio (gm/kg), and wind (mph) in the lower layers of a squall line environment.

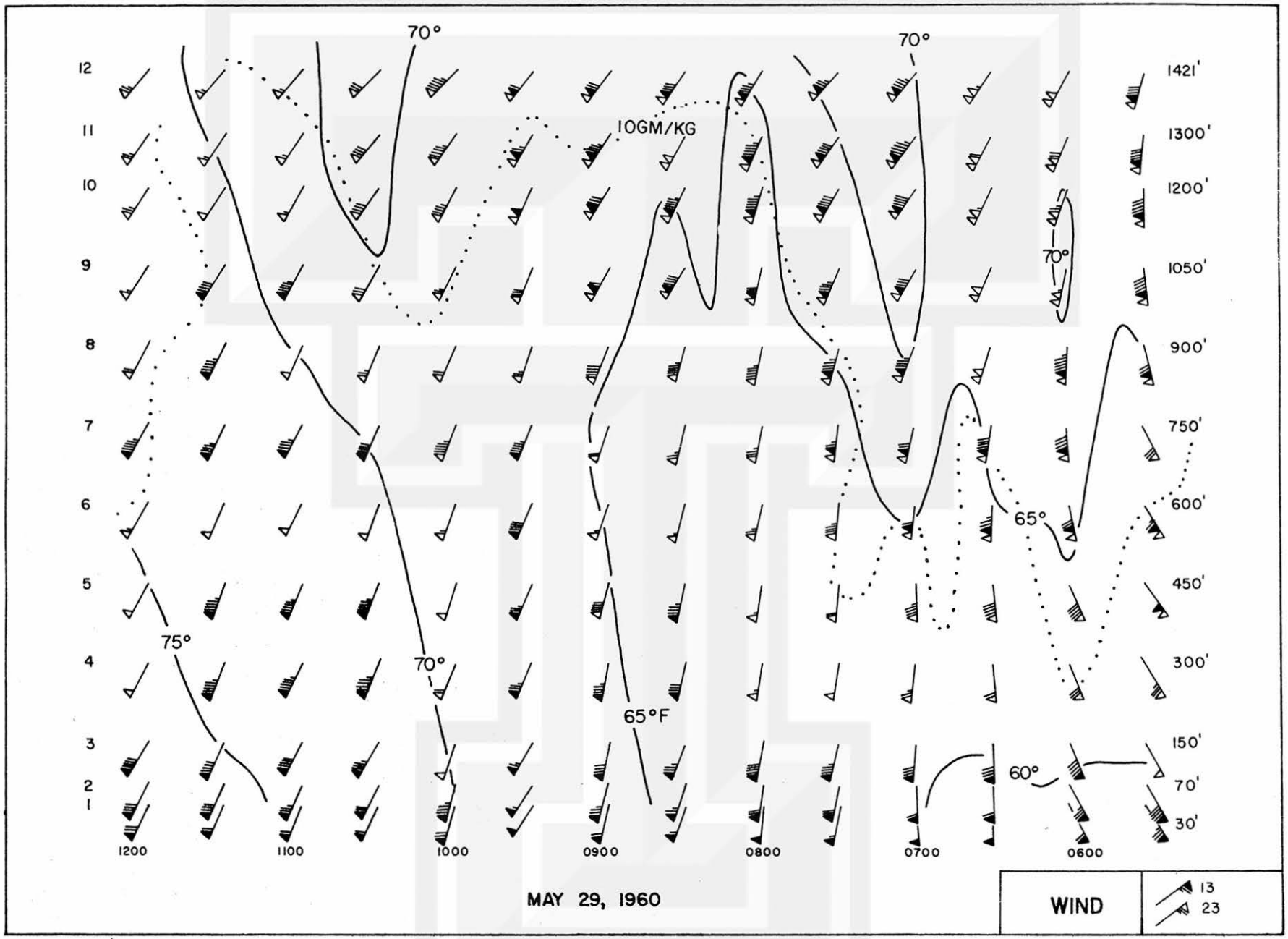

Fig. 18 Time variation of temperature (°F), mixing ratio (gm/kg), and wind (mph) in the lower layers of a post-squall line environment.

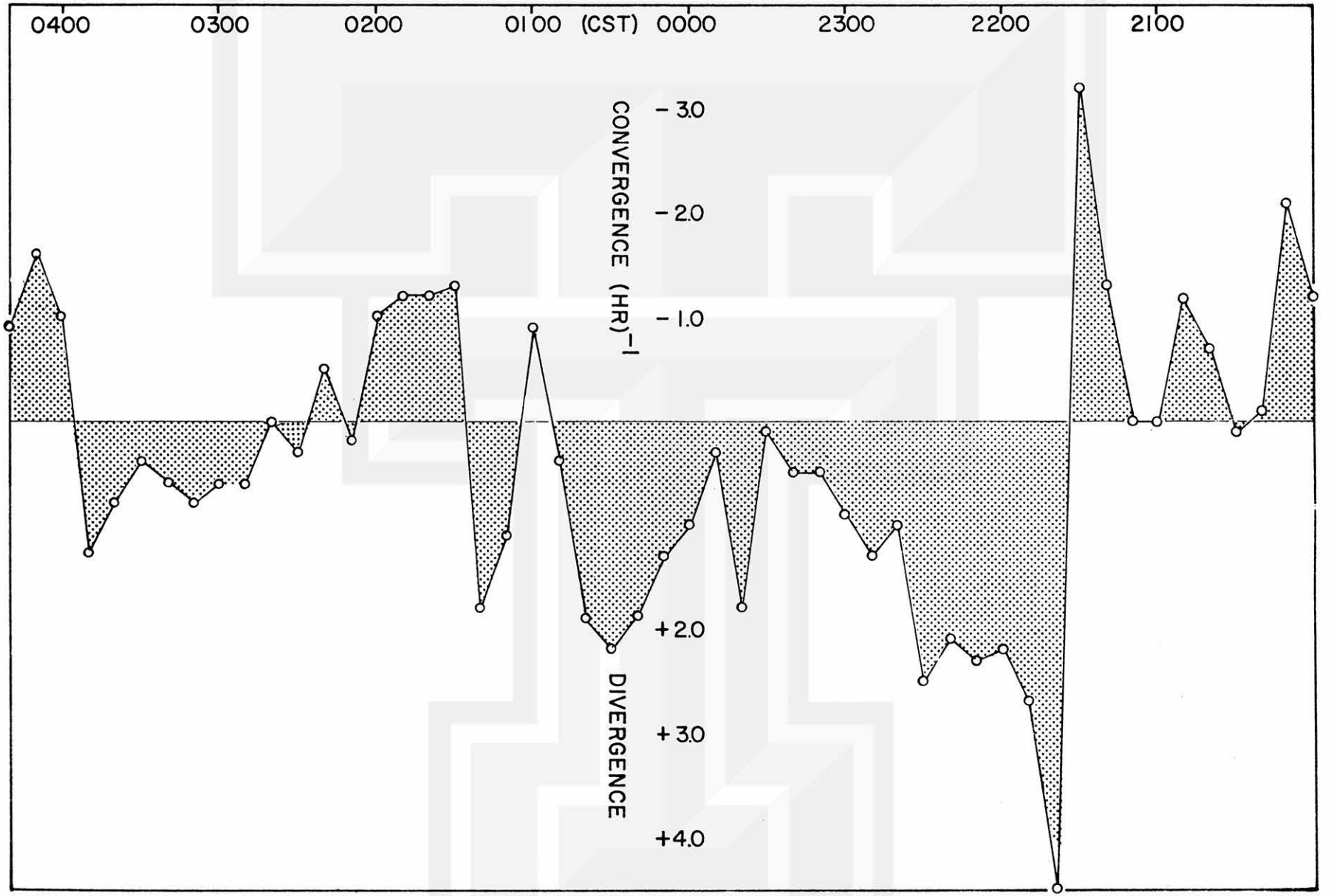

Fig. 19 Time variation (10-minute intervals) of divergence of the surface wind obtained from one-minute averages.

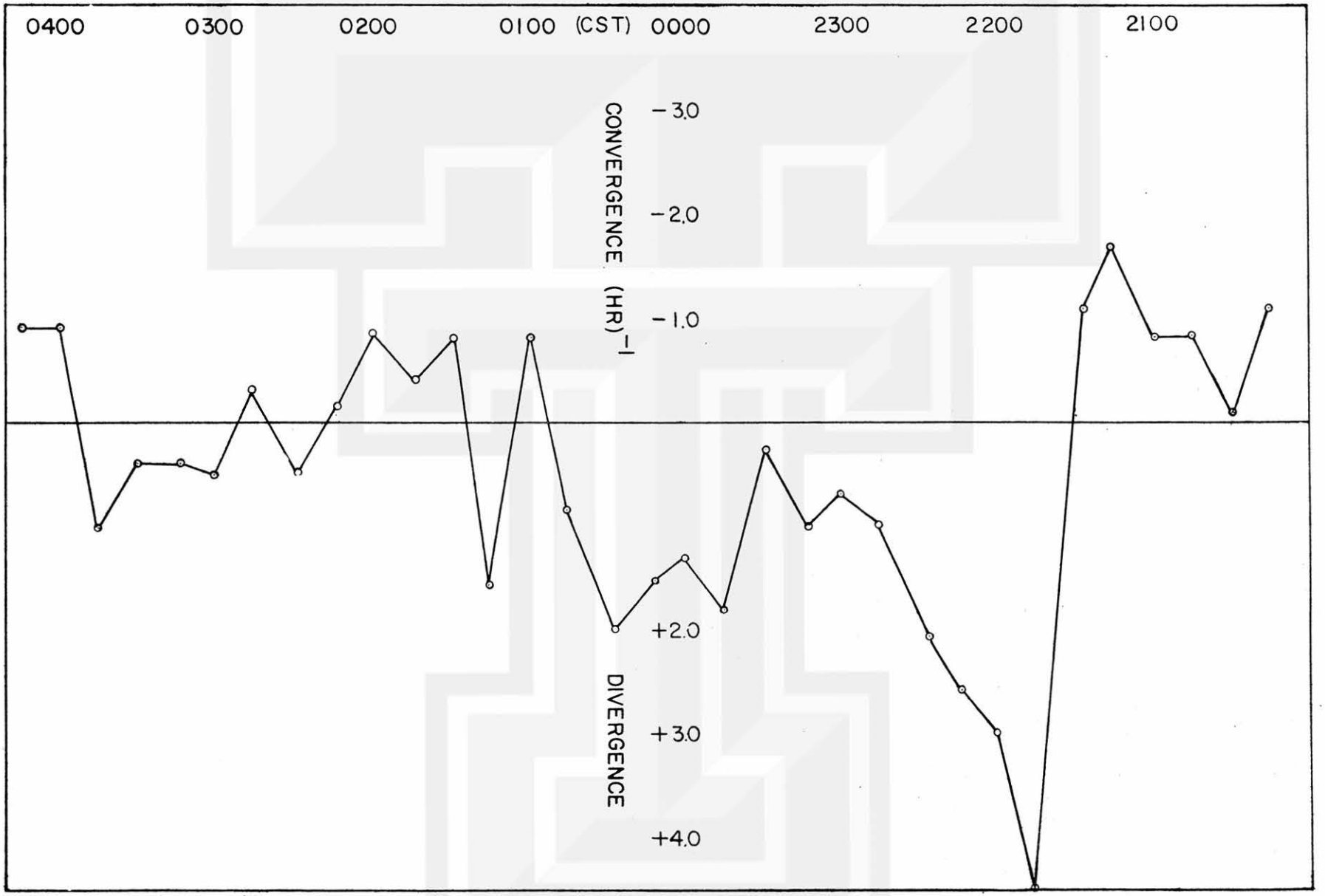

Fig. 20 Time variation (15-minute intervals) of divergence of the surface wind obtained from 10-minute averages.

MESOMETEOROLOGY PROJECT ------- RESEARCH PAPERS
(Continued from front cover)

16. Preliminary Result of Analysis of the Cumulonimbus Cloud of April 21, 1961 - Tetsuya Fujita and James Arnold

17. A Technique for Precise Analysis of Satellite Photographs - Tetsuya Fujita

18. Evaluation of Limb Darkening From TIROS III Radiation Data - S. H. H. Larsen, Tetsuya Fujita, and W. L. Fletcher

19. Synoptic Interpretation of TIROS III Measurements of Infrared Radiation - Finn Pedersen and Tetsuya Fujita

20. TIROS III Measurements of Terrestrial Radiation and Reflected and Scattered Solar Radiation - S. H. H. Larsen, Tetsuya Fujita, and W. L. Fletcher